

# Synchronization in $\mathcal{PT}$ -symmetric optomechanical resonators

Chang-long Zhu,<sup>1</sup> Yu-long Liu,<sup>2</sup> Lan Yang,<sup>3</sup> Yu-xi Liu,<sup>2,4,\*</sup> and Jing Zhang<sup>1,4,†</sup>

<sup>1</sup>*Department of Automation, Tsinghua University, Beijing 100084, P. R. China*

<sup>2</sup>*Institute of Microelectronics, Tsinghua University, Beijing 100084, P. R. China*

<sup>3</sup>*Department of Electrical and Systems Engineering,  
Washington University, St. Louis, MO 63130, USA*

<sup>4</sup>*Center for Quantum Information Science and Technology, BNRist, Beijing 100084, P. R. China*

(Dated: July 18, 2019)

Synchronization has great impacts in various fields such as self-clocking, communication, neural networks, etc. Here we present a mechanism of synchronization for two mechanical modes in two coupled optomechanical resonators by introducing the so-called  $\mathcal{PT}$ -symmetric structure. It is shown that the degree of synchronization between the two far-off-resonant mechanical modes can be increased by decreasing the coupling strength between the two optomechanical resonators. Additionally, when we consider the stochastic noises in the optomechanical resonators, we find that more noises can enhance the degree of synchronization of the system under particular parameter regime. Our results open up the new dimension of research for  $\mathcal{PT}$ -symmetric systems and synchronization.

PACS numbers: 05.45.Xt, 07.10.Cm, 45.50.Wk, 42.65.-k

*Introduction.*—Synchronization is a phenomenon in which two or more systems coordinate and act in the same time with similar behavior. It can be extensively observed in our daily life, such as the chorusing of crickets, flash of fireflies, applauding of audiences, pendulum clocks, firing neurons, and even the life cycle of creatures [1, 2]. As synchronization is a qualitative transition that the rhythms of two or more different objects are adjusted in unison, it also attracts great interest and is widely applied to various fields, such as data communication, time keeping, navigation, cryptography, and neuroscience [3–8].

Due to the recent developments of nano-fabrication techniques, especially those for high-quality-factor on-chip optomechanical resonators [9], it is possible to demonstrate synchronization in on-chip nano-scale platforms [10–14]. For example, in Ref. [12], a pair of closely placed optomechanical resonators with different mechanical frequencies were synchronized by indirect coupling through the coupled optical fields. In Ref. [13], two nanomechanical oscillators separated for about 80  $\mu\text{m}$  were synchronized through the same optical field in an optical racetrack. Moreover, in Ref. [14], master-slave frequency locking was realized between two separated optomechanical oscillators (3.2 km apart) through the light.

In this paper, we show that mechanical oscillations can be synchronized by optomechanical couplings to two coupled optical modes, in which one is active and the other one is passive. Such kinds of systems are called parity-time ( $\mathcal{PT}$ )-symmetric optomechanical systems, which have attracted great attentions in recent years [15–20], and various interesting phenomena have been observed in the systems with  $\mathcal{PT}$ -symmetric structure [15–41]. By

introducing the  $\mathcal{PT}$ -symmetric structure, we observe an interesting phenomenon that the two mechanical modes of the coupled optomechanical resonators tend to oscillate in unison by decreasing the optical coupling strength between them. This observation somewhat conflicts with the normal phenomenon that: the stronger coupling strength between two systems is, the easier the synchronization can be realized. Another counterintuitive phenomenon is observed when we consider the noises acting on the optomechanical resonators. It is shown that more noises will benefit the synchronization process between the two mechanical modes of these two optomechanical resonators.

*Synchronization via  $\mathcal{PT}$ -symmetry.*—As shown in Fig. 1(a), the system we consider here consists of two coupled whispering-gallery-mode (WGM) resonators. The left WGM resonator ( $\mu C_1$ ) is an active one which can be realized, e.g., by  $\text{Er}^{3+}$ -doped silica disk, and the right one ( $\mu C_2$ ) is a passive resonator. Each resonator supports an optical mode  $\alpha_i$  and a mechanical mode  $\beta_i$  ( $i = 1, 2$ ), and the optical coupling strength between  $\alpha_1$  and  $\alpha_2$  is  $\kappa$ . As is well known, although the two mechanical modes  $\beta_1$  and  $\beta_2$ , located in two different resonators, are not directly coupled, these two mechanical modes can be indirectly coupled through the inter-cavity optical coupling and the intra-cavity optomechanical coupling. We elaborate this indirect mechanical coupling in Fig. 1(b). Each WGM resonator is equivalent to a Fabry-Perot cavity, with one fixed mirror and one movable one. The optical modes  $\alpha_1$  and  $\alpha_2$  represent the optical fields in the Fabry-Perot cavities and the mechanical modes  $\beta_1$  and  $\beta_2$  indicate the motions of the movable mirrors. In each equivalent Fabry-Perot cavity, the movable mirror suffers a radiation-pressure force induced by the optical mode  $\alpha_i$  ( $i=1,2$ ). Such a force is proportional to the circulating optical intensity  $|\alpha_i|^2$  in the cavity, which leads to the mechanical motion  $\beta_i$ . In the meanwhile, the movable mirror induces a frequency-shift of the optical mode

\*Electronic address: yuxiliu@mail.tsinghua.edu.cn

†Electronic address: jing-zhang@mail.tsinghua.edu.cn

in the cavity, which influences the dynamics of  $\alpha_i$ . In Fig. 1(b),  $\alpha_1$  ( $\alpha_2$ ) and  $\beta_1$  ( $\beta_2$ ) interact with each other through this kind of radiation-pressure coupling, and  $\alpha_1$  and  $\alpha_2$  are coupled through the evanescent optical fields. Therefore, the mechanical modes  $\beta_1$  and  $\beta_2$  are coupled indirectly by the evanescent optical coupling between  $\alpha_1$  and  $\alpha_2$ .

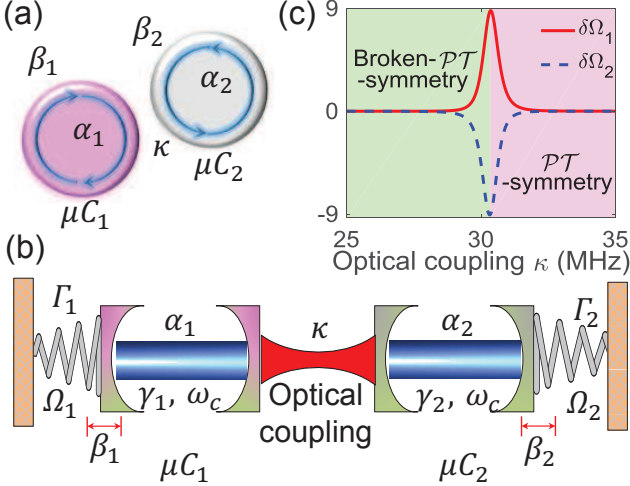


FIG. 1: (color online) Schematic diagram of the optically-coupled  $\mathcal{PT}$  optomechanical system. (a)  $\mu C_1$  denotes an active WGM resonator with gain medium and  $\mu C_2$  is a passive one. (b) The equivalent diagram of the  $\mathcal{PT}$  optomechanical system, where the WGM resonators are replaced by Fabry-Perot cavities with a moveable end mirror and a fixed one. (c) The optically-induced mechanical frequency shifts  $\delta\Omega_{1,2}$  of the two optomechanical resonators versus the optical coupling strength  $\kappa$  both in broken- $\mathcal{PT}$ -symmetric regime and  $\mathcal{PT}$ -symmetric regime.

The  $\mathcal{PT}$ -optomechanical system we consider can be represented by the following equations:

$$\begin{aligned} \dot{\alpha}_1 &= -\Gamma_{\text{op}1}\alpha_1 - i\kappa\alpha_2 - ig_{\text{om}}\alpha_1(\beta_1 + \beta_1^*) + \sqrt{2\gamma_{1\text{ex}}}\epsilon_1, \\ \dot{\alpha}_2 &= -\Gamma_{\text{op}2}\alpha_2 - i\kappa\alpha_1 - ig_{\text{om}}\alpha_2(\beta_2 + \beta_2^*) + \sqrt{2\gamma_{2\text{ex}}}\epsilon_2, \\ \dot{\beta}_1 &= -(\Gamma_{m1} + i\Omega_1)\beta_1 - ig_{\text{om}}|\alpha_1|^2, \\ \dot{\beta}_2 &= -(\Gamma_{m2} + i\Omega_2)\beta_2 - ig_{\text{om}}|\alpha_2|^2, \end{aligned} \quad (1)$$

where  $\Gamma_{\text{op}1} = -\gamma_1 + i\Delta_1$  and  $\Gamma_{\text{op}2} = \gamma_2 + i\Delta_2$ .  $\gamma_i$ ,  $\gamma_{\text{ex}}$ ,  $\Delta_i = \omega_{ci} - \omega_L$ , and  $\epsilon_i$  ( $i = 1, 2$ ) denote the gain (loss) rate of the resonator  $\mu C_i$ , the external damping rate induced by the coupling between the resonator and the input/output fiber-taper, the detuning frequency between the resonance frequency ( $\omega_{ci}$ ) of the cavity mode and the frequency ( $\omega_L$ ) of the driving field, and the amplitude of the driving field, respectively.  $\Omega_i$  and  $\Gamma_{mi}$  represent the frequency and damping rate of the mechanical mode  $\beta_i$ . To simplify our discussion, we assume that the gain cavity  $\mu C_1$  and the lossy cavity  $\mu C_2$  have the same optomechanical coupling strength  $g_{\text{om}}$ . We also assume that the gain rate of  $\mu C_1$  is equal to the damping rate of  $\mu C_2$ , i.e.,  $\gamma_2 = \gamma_1 \equiv \gamma$ , which means that the gain and loss in

the system are well balanced. Additionally, we consider the case of critical coupling such that  $\gamma_{1\text{ex}} = \gamma_{2\text{ex}} = \gamma/2$ , under which there exists a phase transition point, called exceptional point (EP), corresponding to a critical intercavity coupling strength  $\kappa_{\text{EP}} = \gamma$ . When  $\kappa > \kappa_{\text{EP}}$  which is in so-called  $\mathcal{PT}$ -symmetric regime, there exist two non-degenerate optical supermodes with the same damping rate. When  $\kappa \leq \kappa_{\text{EP}}$  which is in so-called broken  $\mathcal{PT}$ -symmetric regime, the two optical supermodes are degenerate but with different damping rates. When the system is far away from EP, the interaction between the optical supermodes and mechanical modes, i.e. the effective radiation-pressure coupling in the supermode picture, is weak. However, this kind of interaction will be greatly enhanced as  $\kappa$  approaches to  $\kappa_{\text{EP}}$ . This results from the amplification of the optomechanical nonlinearity in the vicinity of the exceptional point [16–19].

When the degrees of freedom of the optical modes is adiabatically eliminated under the condition that the optical decay rates are much larger than the mechanical decay rates, such an enhanced optomechanical nonlinearity will induce significant effective frequency shifts  $\delta\Omega_1$  and  $\delta\Omega_2$  for the mechanical modes  $\beta_1$  and  $\beta_2$  in the vicinity of EP. In fact, under the condition that  $g_{\text{om}} \ll |\Delta_1 - \Delta_2| \ll \kappa, \gamma$  and  $\epsilon_1 = \epsilon_2 \equiv \epsilon$ ,  $\delta\Omega_1$  and  $\delta\Omega_2$  near EP can be written as

$$\delta\Omega_1 = -\delta\Omega_2 \approx \frac{2g_{\text{om}}^2\Delta_- \gamma^3(\gamma^2 + \kappa^2)\epsilon^2}{[(\kappa^2 - \gamma^2)^2 + \gamma^2\Delta_-^2]^2}, \quad (2)$$

where  $\Delta_- = \Delta_2 - \Delta_1$ .

Given the system parameters  $\gamma = 30$  MHz,  $\Delta_1 = 4.2$  MHz,  $\Delta_2 = 5$  MHz,  $\Omega_1 = 5$  MHz,  $\Omega_2 = 15$  MHz,  $\Gamma_{m1} = 8$  kHz,  $\Gamma_{m2} = 8$  kHz,  $g_{\text{om}} = 3$  kHz, and  $\epsilon = 70$  MHz $^{1/2}$ , we show in Fig. 2(a) the effective mechanical frequencies  $\Omega_{1,\text{eff}} = \Omega_1 + \delta\Omega_1$  (red-solid curve) and  $\Omega_{2,\text{eff}} = \Omega_2 + \delta\Omega_2$  (blue-dashed curve) of the two resonators versus the optical coupling strength  $\kappa$ , both in broken- $\mathcal{PT}$ -symmetric and  $\mathcal{PT}$ -symmetric regimes. When the system is far away from the exceptional point, the optomechanics-induced mechanical frequency shift  $\delta\Omega_i$  is negligible. However,  $\delta\Omega_i$  will be greatly enhanced such that  $\delta\Omega_i$  is almost comparable with or even larger than  $\Omega_i$ , when  $\kappa$  approaches to  $\kappa_{\text{EP}}$ . These enhanced frequency shifts for the mechanical modes lead to significant modifications of mechanical frequencies  $\Omega_1$  and  $\Omega_2$ , which then make the two mechanical oscillators tend to be resonant with each other, i.e.,  $\Omega_{1,\text{eff}} = \Omega_{2,\text{eff}}$ , and thus synchronize. As is well known, the frequency-mismatch between two synchronized oscillators should be very small in traditional lossy systems [11, 12], i.e.,  $|\Omega_1 - \Omega_2| \ll \Omega_1, \Omega_2$ . However, as shown in Fig. 2, our  $\mathcal{PT}$ -symmetric system can perfectly synchronize two far-off-resonant mechanical oscillators. In fact, as shown in Fig. 2(a), the effective mechanical frequencies of the two optomechanical resonators  $\Omega_{1,\text{eff}}$  and  $\Omega_{2,\text{eff}}$  coincide with each other when  $\kappa$  approaches to  $\kappa_{\text{EP}}$ .

In addition, we find an anti-intuitive phenomenon that *weaker* coupling between two optomechanical resonators may be *helpful* for synchronization for our  $\mathcal{PT}$  optomechanical system. In fact, as shown in Fig. 2(a), in the  $\mathcal{PT}$ -symmetric regime (the pink region), when the coupling strength  $\kappa$  between two resonators is *decreased*, the effective mechanical frequencies of the two resonators tend to coincide with each other, which means that  $\beta_1$  and  $\beta_2$  are inclined to oscillate in unison with weaker coupling strength  $\kappa$  in the  $\mathcal{PT}$ -symmetric regime. The broken- $\mathcal{PT}$ -symmetric regime is the normal regime where stronger coupling between the two optomechanical resonators make the two mechanical modes  $\beta_1$  and  $\beta_2$  be inclined to be synchronized. We can more easily see this phenomenon by plotting the spectra of the normalized mechanical displacements of the two optomechanical resonators  $x_1 = (\beta_1 + \beta_1^*)/2$  (the red solid curve) and  $x_2 = (\beta_2 + \beta_2^*)/2$  (the blue dashed curve) in Figs. 2 (c) and (d), where  $\kappa$  is increased from 2 MHz to 29.86 MHz in Fig. 2 (c), and is decreased from 50 MHz to 30.81 MHz in Fig. 2 (d). As shown in Fig. 2(c), with the increase of the inter-cavity coupling strength  $\kappa$  in the broken- $\mathcal{PT}$ -symmetric regime, the Lorentz spectra of  $x_1$  (the red-solid curve) and  $x_2$  (the blue-dashed curve) get closer and finally coincide with each other, which means that the two mechanical modes are resonant. However, contrary to our intuition, the resonant peaks of  $x_1$  and  $x_2$  get closer with decreasing  $\kappa$  in the  $\mathcal{PT}$ -symmetric regime as shown in Fig. 2(d). This anti-intuitive phenomenon comes from the fact that synchronization only takes place when we approach EP for two far-off-resonant mechanical modes. In fact, as shown in Eq. (2), the optomechanically-induced mechanical frequency-shifts depend not only on the optical coupling strength  $\kappa$  but also on the optomechanical coupling strength. When we approach EP in the  $\mathcal{PT}$ -symmetric regime, the effective optomechanical coupling strength will be greatly enhanced [16–19] although the optical coupling strength  $\kappa$  is decreased. The increase of the effective optomechanical coupling strength compensates the decrease of the optical coupling strength, which finally leads to the great modification of the effective mechanical frequencies of the resonators.

We can also understand what we observe in another alternative way by which we can adiabatically eliminate the degrees of freedom of the optical modes and obtain an effective coupling strength  $\kappa_{\text{mech}}$  between the two mechanical modes  $\beta_1$  and  $\beta_2$  as

$$\kappa_{\text{mech}} \approx \frac{4g_{\text{om}}^2 \gamma^3 \kappa^2 \Delta_- \epsilon^2}{[(\kappa^2 - \gamma^2)^2 + \gamma^2 \Delta_-^2]^2}. \quad (3)$$

As shown in Fig. 2(b),  $\kappa_{\text{mech}}$  takes maximum when the optical coupling strength approaches EP, under which a better synchronization effects can be obtained.

To give more insights into the phenomena shown by us, we plot in Fig. 3(a) the cross-correlation function  $M_{cc}$  between the two mechanical displacements  $x_1$  and  $x_2$  with

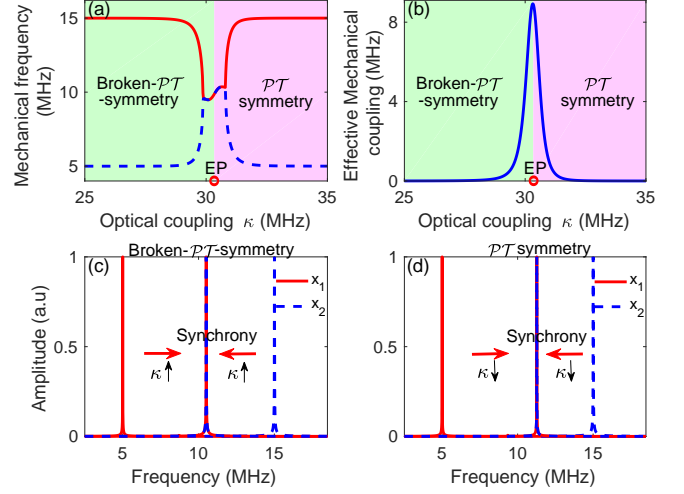


FIG. 2: (color online) (a) The effective mechanical frequencies  $\Omega_{1,\text{eff}}$  and  $\Omega_{2,\text{eff}}$  versus the optical coupling strength  $\kappa$ , where the blue solid (red dashed) curve represents the frequency of  $\beta_1$  ( $\beta_2$ ), the light green (pink) area is the broken- $\mathcal{PT}$ -symmetric ( $\mathcal{PT}$ -symmetric) regime. (b) The effective coupling strength  $\kappa_{\text{mech}}$  between two mechanical modes versus the optical coupling strength  $\kappa$  in broken- $\mathcal{PT}$ -symmetric regime and  $\mathcal{PT}$ -symmetric regime. (c) Spectrograms of mechanical modes  $x_1$  and  $x_2$  with increasing optical coupling strength  $\kappa$  in the broken-  $\mathcal{PT}$ -symmetric regime. Here,  $\kappa \uparrow$  and  $\kappa \downarrow$  denote the increase and decrease of  $\kappa$ . (d) Spectrograms of mechanical modes  $x_1$  and  $x_2$  with decreasing optical coupling strength  $\kappa$  in the  $\mathcal{PT}$ -symmetric regime, in which weaker coupling strength  $\kappa$  makes the two resonators easier to be synchronized.

different inter-cavity optical coupling strength  $\kappa$ , where  $M_{cc}$  is defined as [42, 43]

$$M_{cc} = \max_{0 < t < +\infty} \frac{1}{\sqrt{\phi_1 \phi_2}} \int_0^{+\infty} x_1(\tau - t) x_2(\tau) d\tau, \\ \phi_i = \int_0^{+\infty} x_i^2(\tau) d\tau. \quad (4)$$

As shown in Fig. 3(a), in the  $\mathcal{PT}$ -symmetric regime, smaller  $\kappa$  induces higher value of  $M_{cc}$  (the red solid curve), and  $M_{cc}$  reaches the maximum value (the unit) as  $\kappa$  decreases and approaches EP, which means that the two mechanical displacements  $x_1$  and  $x_2$  tend to be synchronized with the decrease of the inter-cavity coupling strength. However, in the broken- $\mathcal{PT}$  symmetric regime (the blue dashed curve), the cross-correlation function increases and tends to unit with the increase of  $\kappa$ , which means that stronger inter-cavity coupling strength will be helpful for synchronization as we expect.

*Noise-enhanced synchronization.*—We now study the effects of the stochastic noises on our  $\mathcal{PT}$ -symmetric system. Two independently-identically-distributed Gaussian white noises  $\xi_{1,2}$  are introduced for the two optical modes  $\alpha_{1,2}$ , such that  $\langle \xi_i(t) \xi_j(t + \tau) \rangle = 2D\delta_{ij}\delta(\tau)$ , where  $D$  is the intensity of the noises. We present the nu-

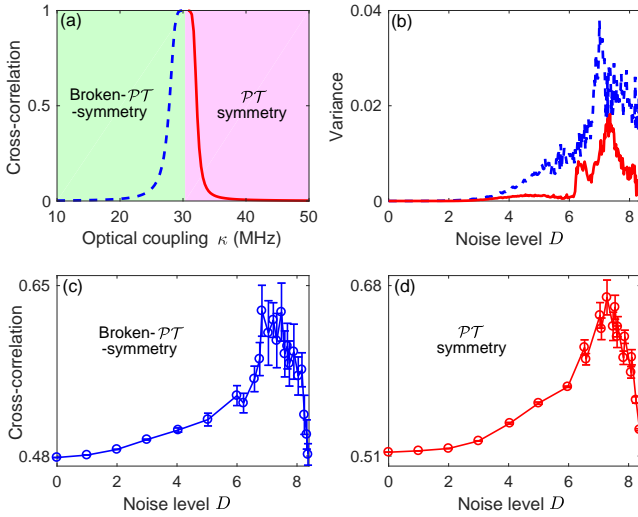


FIG. 3: (color online) (a) Numerical results of cross-correlation  $M_{cc}$  with different values of  $\kappa$  in broken- $\mathcal{PT}$ -symmetric and  $\mathcal{PT}$ -symmetric regimes. (b) The variances of  $M_{cc}$  versus noise level  $D$ , where the blue dashed line represents the variance of cross-correlation in (c), and the red solid line corresponds to the variance in (d). (c) Effects of the stochastic noises on  $M_{cc}$  with respect to different stochastic noise intensity  $D$  in broken  $\mathcal{PT}$ -symmetric regime with  $\kappa = 27.76$  MHz. (d) Effects of the stochastic noises on  $M_{cc}$  versus different  $D$  in  $\mathcal{PT}$ -symmetric regime with  $\kappa = 32.19$  MHz.

merical results of the cross-correlation function  $M_{cc}$  between the two mechanical oscillators in Figs. 3(b) and (c) by changing the noise strength  $D$  and fixing other parameters both in broken- $\mathcal{PT}$ -symmetric and  $\mathcal{PT}$ -symmetric regimes. It can be seen that  $M_{cc}$  is enhanced with increasing noise intensity  $D$  both in broken- $\mathcal{PT}$ -symmetric and  $\mathcal{PT}$ -symmetric regime, reaches the maximal values at particular noise level, and then decreases at higher noise intensity. It means that synchronization process may benefit from noises [44–51] in our optomechanical  $\mathcal{PT}$ -symmetric system. To interpret what we observe, we can see that the noise will randomly shift the frequencies of the mechanical modes, especially when we approach EP where the effects of noise are enhanced [52–55]. Since the frequencies of the two mechanical modes are far-separated, these random frequency shifts may decrease the difference between the frequencies of the two mechanical modes in a certain probability with increasing noise strength  $D$ , and thus increase the cross-correlation function  $M_{cc}$ . When we increase the noise strength  $D$  further, the noise will be strong enough to destroy the periodic oscillation of single mechanical oscillator, and thus decrease the degree of synchronization between the

two mechanical oscillators. This interpretation can also be confirmed by checking the variance of  $M_{cc}$  versus the noise strength  $D$  (Fig. 3(b)). The variance of  $M_{cc}$  first increases with increasing noise strength  $D$  (note that  $M_{cc}$  increases at the same time), which means that more noises enter the system although  $M_{cc}$  is increased. The variance of  $M_{cc}$  then decreases when we increase  $D$  further, because the value of  $M_{cc}$  is too small in this case and the noise-induced fluctuations in  $M_{cc}$  are suppressed.

Furthermore, we consider the effects of the thermal noises in the two mechanical modes by calculating the normalized correlation function  $R$  between the two mechanical modes [56] (see supplementary II B). In the broken- $\mathcal{PT}$ -symmetric regime with optical coupling strength  $\kappa = 27.79$  MHz, the normalized correlation function  $R$  is equal to 0.54, which is larger than 0.48 where we ignore the thermal noises. Similarly, in the  $\mathcal{PT}$ -symmetric regime with optical coupling strength  $\kappa = 32.19$  MHz,  $R$  is equal to 0.59 which is also larger than 0.51 where we ignore the thermal noises. This indicates that the thermal noises in the mechanical modes can also benefit the synchronization between the two mechanical modes in our optomechanical  $\mathcal{PT}$ -symmetric system.

*Conclusion.*—We have shown that the mechanical motions of two coupled  $\mathcal{PT}$ -symmetric optomechanical resonators with far-off-resonant mechanical frequencies can be synchronized when the system approaches EP. In particular, in the  $\mathcal{PT}$ -symmetric regime, the two mechanical modes are easier to be synchronized with less optical coupling strength between the two optomechanical resonators. Additionally, it is shown that noises will be enhanced in the vicinity of EP in our system, and the enhanced noises will benefit the synchronization process if only the strengths of the noises are not too strong. Our study opens up new dimension of research for  $\mathcal{PT}$ -symmetric optomechanical system for possible applications such as metrology, cooling, and communication. It also gives new perspectives for synchronization in optomechanical systems.

JZ is supported by the NSFC under Grant Nos. 61622306, 11674194. YXL and JZ are supported by the National Basic Research Program of China (973 Program) under Grant No. 2014CB921401, the Tsinghua University Initiative Scientific Research Program, and the Tsinghua National Laboratory for Information Science and Technology (TNList) Cross-discipline Foundation. JZ is also supported by the Youth Innovation Fund of Beijing National Research Center for Information Science and Technology (BNRist). LY is supported by the NSF grant No. EFMA1641109, ARO grant No. W911NF1210026 and ARO grant No. W911NF1710189.

[1] A. S. Pikovsky, M. Rosenblum, and J. Kurths, *Synchronization—A Unified Approach to Nonlinear Science*

(Cambridge University Press, Cambridge, UK, 2001).  
[2] L. Glass, M. C. Mackey, *From Clocks to Chaos: The*

- Rhythms of Life (Princeton Univ. Press, Princeton, NJ, 1988).
- [3] A. T. Winfree, The Geometry of Biological Time (Springer, New York, ed. 2, 2001).
- [4] A. Goldbeter, Biochemical Oscillations and Cellular Rhythms: The Molecular Bases of Periodic and Chaotic Behaviour (Cambridge Univ. Press, Cambridge, 1996).
- [5] A. F. Taylor, M. R. Tinsley, F. Wang, Z. Y. Huang, and K. Showalter, Dynamical quorum sensing and synchronization in large populations of chemical oscillators, *Science* **323**, 614 (2009).
- [6] S. H. Strogatz, Sync: The Emerging Science of Spontaneous Order (Hyperion, New York, 2003), 1st ed.
- [7] S. C. Manrubia, A. S. Mikhailov, D. H. Zanette, Emergence of Dynamical Order: Synchronization Phenomena in Complex Systems (World Scientific, Singapore, 2004).
- [8] S. Bagni, Synchronization of Digital Telecommunications Networks (Wiley, Chichester, 2002).
- [9] M. Aspelmeyer, T. J. Kippenberg, and F. Marquardt, Cavity optomechanics, *Rev. Mod. Phys.* **86**, 1391 (2014).
- [10] C. A. Holmes, C. P. Meaney, and G. J. Milburn, Synchronization of many nanomechanical resonators coupled via a common cavity field, *Phys. Rev. E* **85**, 066203 (2012).
- [11] T. Li, T. Y. Bao, Y. L. Zhang, C. L. Zou, X. B. Zou, and G. C. Guo, Long-distance synchronization of unidirectionally cascaded optomechanical systems, *Opt. Exp.* **24**, 12338 (2016).
- [12] M. Zhang, G. S. Wiederhecker, S. Manipatruni, A. Barnard, P. McEuen, and M. Lipson, Synchronization of micromechanical oscillators using light, *Phys. Rev. Lett.* **109**, 233906 (2012).
- [13] M. Bagheri, M. Poot, L. Fan, F. Marquardt, and H. X. Tang, Photonic cavity synchronization of nanomechanical oscillators, *Phys. Rev. Lett.* **111**, 213902 (2013).
- [14] S. Y. Shah, M. Zhang, R. Rand, and M. Lipson, Master-slave locking of optomechanical oscillators over a long distance, *Phys. Rev. Lett.* **114**, 113602 (2015).
- [15] H. Xu, D. Mason, L. Jiang, and G. E. Harris, Topological energy transfer in an optomechanical system with exceptional points, *Nature* **537**, 80 (2016).
- [16] H. Jing, S. K. Özdemir, X. Y. L, J. Zhang, L. Yang, and F. Nori, PT-Symmetric phonon laser, *Phys. Rev. Lett.* **113**, 053604 (2014).
- [17] Z. P. Liu, J. Zhang, S. K. Özdemir, B. Peng, H. Jing, X. Y. Lü, C. W. Li, L. Yang, F. Nori, and Y. X. Liu, Metrology with PT-symmetric cavities: enhanced sensitivity near the PT-phase transition, *Phys. Rev. Lett.* **117**, 110802 (2016).
- [18] H. Jing, S. K. Özdemir, Z. Geng, J. Zhang, X. Y. L, B. Peng, L. Yang, and F. Nori, Optomechanically-induced transparency in parity-time-symmetric microresonators, *Sci. Rep.* **5**, 9663 (2015).
- [19] J. Zhang, P. Bo, S. K. Özdemir, Y. X. H. Jing, X. Y. Lü, Y. L. Liu, L. Yang, and F. Nori, Giant nonlinearity via breaking parity-time symmetry: a route to low-threshold phonon diodes, *Phys. Rev. B* **92**, 115407 (2015).
- [20] X. Y. Lü, H. Jing, J. Y. Ma, and Y. Wu, PT-symmetry-breaking Chaos in Optomechanics, *Phys. Rev. Lett.* **114**, 253601 (2015).
- [21] C. M. Bender and S. Boettcher, Real spectra in non-Hermitian Hamiltonians having PT symmetry, *Phys. Rev. Lett.* **80**, 5243 (1998).
- [22] C. M. Bender, Making sense of non-Hermitian Hamiltonians, *Rep. Prog. Phys.* **70**, 947 (2007).
- [23] G. S. Agarwal and K. Qu, Spontaneous generation of photons in transmission of quantum fields in  $\mathcal{PT}$ -symmetric optical systems, *Phys. Rev. A* **85**, 031802 (2012).
- [24] A. Mostafazadeh, Pseudo-Hermiticity versus PT symmetry: the necessary condition for the reality of the spectrum of a non-Hermitian Hamiltonian, *J. Math. Phys.* **43**, 205 (2002).
- [25] B. Peng, S. K. Özdemir, F. C. Lei, F. Monifi, M. Giannfreda, G. L. Long, S. H. Fan, F. Nori, C. M. Bender, and L. Yang, Parity-time-symmetric whispering-gallery microcavities, *Nat. Phys.* **10**, 394 (2014).
- [26] L. Feng, Z. J. Wong, R. M. Ma, Y. Wang, and X. Zhang, Singlemode laser by parity-time symmetry breaking, *Science* **346**, 972 (2014).
- [27] H. Hodaei, M. A. Miri, M. Heinrich, D. N. Christodoulides, and M. Khajavikhan, Parity-time-symmetric microring lasers, *Science* **346**, 975 (2014).
- [28] A. Guo, G. J. Salamo, D. Duchesne, R. Morandotti, M. Volatier-Ravat, V. Aimez, G. A. Siviloglou, and D. N. Christodoulides, Observation of PT-symmetry breaking in complex optical potentials, *Phys. Rev. Lett.* **103**, 093902 (2009).
- [29] C. E. Rüter, K. G. Makris, R. El-Ganainy, D. N. Christodoulides, M. Segev, and D. Kip, Observation of parity-time symmetry in optics, *Nat. Phys.* **6**, 192 (2010).
- [30] H. Ramezani, T. Kottos, R. El-Ganainy, and D. N. Christodoulides, Unidirectional nonlinear PT-symmetric optical structures, *Phys. Rev. A* **82**, 043803 (2010).
- [31] Z. Lin, H. Ramezani, T. Eichelkraut, T. Kottos, H. Cao, and D. N. Christodoulides, Unidirectional invisibility induced by PT-symmetric periodic structures, *Phys. Rev. Lett.* **106**, 213901 (2011).
- [32] L. Feng, M. Ayache, J. Huang, Y. L. Xu, M. H. Lu, Y. F. Chen, Y. Fainman, and A. Scherer, Nonreciprocal light propagation in a silicon photonic circuit, *Science* **333**, 729 (2011).
- [33] A. Regensburger, C. Bersch, M. A. Miri, G. Onishchukov, D. N. Christodoulides, and U. Peschel, Parity-time synthetic photonic lattices, *Nature (London)* **488**, 167 (2012).
- [34] L. Chang, X. S. Jiang, S. Y. Hua, C. Yang, J. M. Wen, L. Jiang, G. Y. Li, G. Z. Wang, and M. Xiao, Parity-time symmetry and variable optical isolation in active-passive-coupled microresonators, *Nat. Photonics.* **8**, 524 (2014).
- [35] B. Peng, S. K. Özdemir, S. Rotter, H. Yilmaz, M. Liertzer, F. Monifi, C. M. Bender, F. Nori, and L. Yang, Loss induced suppression and revival of lasing, *Science* **346**, 328 (2014).
- [36] J. Schindler, A. Li, M. C. Zheng, F. M. Ellis, and T. Kottos, Experimental study of active LRC circuits with PT symmetries. *Phys. Rev. A* **84**, 040101(R) (2011).
- [37] C. T. West, T. Kottos, and T. Prosen, PT-symmetric wave chaos. *Phys. Rev. Lett.* **104**, 054102 (2015).
- [38] J. Wiersig, Enhancing the sensitivity of frequency and energy splitting detection by using exceptional points: application to microcavity sensors for single-particle detection. *Phys. Rev. Lett.* **112**, 203901 (2014).
- [39] W. Chen, S. K. Ozdemir, G. Zhao, J. Wiersig, and L. Yang, Exceptional points enhance sensing in an optical microcavity, *Nature* **548**, 192-196 (2017).
- [40] H. Hodaei, A. U. Hassan, S. Wittek, H. Garcia-Gracia, R.

- El-Ganainy, D. N. Christodoulides, and M. Khajavikhan, Enhanced sensitivity at higher-order exceptional points, *Nature* **548**, 187-191 (2017).
- [41] J. Doppler, A. A. Mailybaev, J. Bohm, U. Kuhl, A. Girschik, F. Libisch, T. J. Milburn, P. Rabl, N. Moiseyev, and S. Rotter, Dynamically encircling an exceptional point for asymmetric mode switching, *Nature* **537**, 76-79 (2016).
- [42] R. N. Bracewell, *The Fourier Transform and Its Applications* (McGraw-Hill, New York, 1978).
- [43] L. R. Rabiner and R. W. Schafer, *Digital Processing of Speech Signals* (Prentice-Hall, Englewood Cliffs, NJ, 1978).
- [44] A. Neiman, Synchronizationlike phenomena in coupled stochastic bistable systems, *Phys. Rev. E* **49**, 3484 (1994).
- [45] S. K. Han, T. G. Yim, D. E. Postnov and O. V. Sosnovtseva, Interacting coherence resonance oscillators, *Phys. Rev. Lett.* **83**, 1771 (1999).
- [46] A. Neiman, L. Schimansky-Geier, A. Cornell-Bell, and F. Moss, Noise-enhanced phase synchronization in excitable media, *Phys. Rev. Lett.* **83**, 4896 (1999).
- [47] H. Nakao, K. Arai, and Y. Kawamura, Noise-induced synchronization and clustering in ensembles of uncoupled limit-cycle oscillators, *Phys. Rev. Lett.* **98**, 184101 (2007).
- [48] K. H. Nagai and H. Kori, Noise-induced synchronization of a large population of globally coupled nonidentical oscillators, *Phys. Rev. E* **81**, 065202 (2010).
- [49] Y. M. Lai and M. A. Porter, Noise-induced synchronization, desynchronization, and clustering in globally coupled nonidentical oscillators, *Phys. Rev. E* **88**, 012905 (2013).
- [50] C. S. Zhou and J. Kurths, Noise-induced Phase synchronization and synchronization transitions in chaotic oscillators, *Phys. Rev. Lett.* **88** 230602 (2002).
- [51] D. H. He, P. L. Shi, and L. Stone, Noise-induced synchronization in realistic models, *Phys. Rev. E* **67**, 027201 (2003).
- [52] H. Schomerus, Quantum noise and self-sustained radiation of PT-symmetric systems, *Phys. Rev. Lett.* **104**, 233601 (2010).
- [53] S.-Y. Lee, J.-W. Ryu, J.-B. Shim, S.-B. Lee, S. W. Kim, and K. An, Divergent Petermann factor of interacting resonances in a stadium-shaped microcavity, *Phys. Rev. A* **78**, 015805 (2008).
- [54] G. Yoo, H.-S. Sim, and H. Schomerus, Quantum noise and mode nonorthogonality in non-Hermitian PT-symmetric optical resonators, *Phys. Rev. A* **84**, 063833 (2011).
- [55] J. Zhang, B. Peng, S. K. Ozdemir, S. Rotter, K. Pichler, D. Krimer, G. Zhao, F. Nori, Y.-X. Liu, and L. Yang, A phonon laser operating at the exceptional point, *Nat. Photonics* **12**, 479 (2018). *Photonics*.
- [56] H. Risken, *The Fokker-Planck Equation: Methods of Solution and Applications*, 2nd ed. (Springer, Berlin, 1989).

# Supplement to “Synchronization in $\mathcal{PT}$ -symmetric optomechanical resonators”

Chang-long Zhu, Yu-long Liu, Lan Yang, Yu-xi Liu, and Jing Zhang

This supplement provides additional analysis and derivations on the following topics: (I) mechanism of the synchronization in  $\mathcal{PT}$ -symmetric optomechanical system; (II) noise-enhanced synchronization in  $\mathcal{PT}$ -symmetric optomechanical system.

## I. MECHANISM OF SYNCHRONIZATION IN $\mathcal{PT}$ -SYMMETRIC OPTOMECHANICAL SYSTEM

The  $\mathcal{PT}$ -symmetric optomechanical system considered is composed of two coupled optomechanical resonators. One of these two optomechanical resonators is with an active optical mode, and the other one is with a passive optical mode. The dynamical equations of the system can be written as

$$\begin{aligned}\dot{\alpha}_1 &= (\gamma_1 - i\Delta_1)\alpha_1 - i\kappa\alpha_2 - ig_{om}\alpha_1(\beta_1 + \beta_1^*) + \sqrt{2\gamma_{1ex}}\epsilon_1, \\ \dot{\alpha}_2 &= -(\gamma_2 + i\Delta_2)\alpha_2 - i\kappa\alpha_1 - ig_{om}\alpha_2(\beta_2 + \beta_2^*) + \sqrt{2\gamma_{2ex}}\epsilon_2, \\ \dot{\beta}_1 &= -(\Gamma_{m1} + i\Omega_1)\beta_1 - ig_{om}|\alpha_1|^2, \\ \dot{\beta}_2 &= -(\Gamma_{m2} + i\Omega_2)\beta_2 - ig_{om}|\alpha_2|^2,\end{aligned}\quad (1)$$

where  $\alpha_1$  ( $\alpha_2$ ) is the active (passive) optical mode of the first (second) optomechanical resonator, and  $\beta_1$  ( $\beta_2$ ) is the corresponding mechanical mode.  $\gamma_i$  is the gain or loss rate of the optical mode  $\alpha_i$ .  $\epsilon_i$  and  $\Delta_i$  are the strength of the driving field and the detuning frequency between the driving field and the optical mode.  $\Gamma_{mi}$  and  $\Omega_i$  correspond to the damping rate and frequency of the mechanical mode  $\beta_i$ .  $\kappa$  is the coupling strength between two optical modes  $\alpha_1$  and  $\alpha_2$ .  $g_{om}$  is the optomechanical coupling strength.

### A. The optical structure of the $\mathcal{PT}$ -symmetric optomechanical system

By taking  $\dot{\alpha}_{1,2} = \dot{\beta}_{1,2} = 0$ , we can obtain the stationary states of the optical and mechanical modes which satisfies the following equations

$$\begin{aligned}(\gamma_1 - i\Delta_1)\alpha_{1s} - i\kappa\alpha_{2s} - ig_{om}\alpha_{1s}(\beta_{1s} + \beta_{2s}^*) + \sqrt{2\gamma_{1ex}}\epsilon_1 &= 0, \\ -(\gamma_2 + i\Delta_2)\alpha_{2s} - i\kappa\alpha_{1s} - ig_{om}\alpha_{2s}(\beta_{2s} + \beta_{1s}^*) + \sqrt{2\gamma_{2ex}}\epsilon_2 &= 0, \\ -(\Gamma_{m1} + i\Omega_1)\beta_{1s} - ig_{om}|\alpha_{1s}|^2 &= 0, \\ -(\Gamma_{m2} + i\Omega_2)\beta_{2s} - ig_{om}|\alpha_{2s}|^2 &= 0.\end{aligned}$$

By solving the above equations and substituting these stationary states into Eq. (1), we have

$$\begin{aligned}\dot{\alpha}_1 &= [\gamma_1 - i(\Delta_1 + \Delta_{1s})]\alpha_1 - i\kappa\alpha_2 + \sqrt{2\gamma_{1ex}}\epsilon_1, \\ \dot{\alpha}_2 &= [-\gamma_2 - i(\Delta_2 + \Delta_{2s})]\alpha_2 - i\kappa\alpha_1 + \sqrt{2\gamma_{2ex}}\epsilon_2,\end{aligned}\quad (2)$$

where

$$\begin{aligned}\Delta_{1s} &= -\frac{2\Omega_1 g_{om}^2}{\Gamma_{m1}^2 + \Omega_1^2} |\alpha_{1s}|^2, \\ \Delta_{2s} &= -\frac{2\Omega_2 g_{om}^2}{\Gamma_{m2}^2 + \Omega_2^2} |\alpha_{2s}|.\end{aligned}$$

Based on Eq. (2), we can calculate the eigenfrequencies of the optical supermodes as

$$\begin{aligned}\omega_{o+} &= \frac{\gamma_1 - \gamma_2}{2} - i\frac{\Delta_1 + \Delta_{1s} + \Delta_2 + \Delta_{2s}}{2} + \sqrt{\left[\frac{\gamma_1 + \gamma_2}{2} + i\left(\frac{\Delta_2 + \Delta_{2s}}{2} - \frac{\Delta_1 + \Delta_{1s}}{2}\right)\right]^2 - \kappa^2}, \\ \omega_{o-} &= \frac{\gamma_1 - \gamma_2}{2} - i\frac{\Delta_1 + \Delta_{1s} + \Delta_2 + \Delta_{2s}}{2} - \sqrt{\left[\frac{\gamma_1 + \gamma_2}{2} + i\left(\frac{\Delta_2 + \Delta_{2s}}{2} - \frac{\Delta_1 + \Delta_{1s}}{2}\right)\right]^2 - \kappa^2}.\end{aligned}$$

In our optomechanical system with balanced gain and loss, these eigenvalues can be approximated under the condition that  $|(\Delta_2 + \Delta_{2s}) - (\Delta_1 + \Delta_{1s})| \ll \gamma_1, \gamma_2, \kappa$  as

$$\begin{aligned}\omega_{o+} &= -i \frac{\Delta_1 + \Delta_{1s} + \Delta_2 + \Delta_{2s}}{2} + \sqrt{\gamma^2 - \kappa^2}, \\ \omega_{o-} &= -i \frac{\Delta_1 + \Delta_{1s} + \Delta_2 + \Delta_{2s}}{2} - \sqrt{\gamma^2 - \kappa^2},\end{aligned}\quad (3)$$

where  $\gamma_1 = \gamma_2 = \gamma$ . We can see from Eq. (3) that there exists a phase transition point, called exceptional point (EP), when  $\kappa = \kappa_{EP} = \gamma$ . Under the strong intercavity coupling regime such that  $\kappa > \kappa_{EP}$ , the real parts of the two eigenfrequencies  $\omega_{o\pm}$  are the same and the imaginary parts of  $\omega_{o\pm}$  are different, which corresponds to a mode-splitting of the optical supermodes with the same damping rates. We call it  $\mathcal{PT}$ -symmetric regime. In contrast, when the intercavity coupling strength is weak enough such  $\kappa < \kappa_{EP}$ , the real parts of  $\omega_{o\pm}$  are different while the imaginary parts of  $\omega_{o\pm}$  are the same, which corresponds to two degenerate optical supermodes with different damping rates. We call it broken-  $\mathcal{PT}$ -symmetric regime. Given the system parameters  $\gamma_1 = \gamma_2 = 30$  MHz,  $\gamma_{1ex} = \gamma_{2ex} = 15$  MHz,  $\Delta_1 = 4.2$  MHz,  $\Delta_2 = 5$  MHz,  $\Omega_1 = 5$  MHz,  $\Omega_2 = 15$  MHz,  $\Gamma_{m1} = 8$  kHz,  $\Gamma_{m2} = 8$  kHz,  $g_{om} = 3$  kHz, and  $\epsilon_1 = \epsilon_2 = 70$  MHz $^{1/2}$ , the simulation results of the mode splitting and linewidth of the optical supermodes are shown in Figs. 1 (a) and (b).

It should be pointed out that the degeneracy of the optical supermodes at the exceptional point will be broken by the optomechanical coupling given by  $g_{om}$  and the asymmetric optical detuning frequency  $\Delta_- = |\Delta_2 - \Delta_1| \neq 0$ , as shown in Figs. 1 (a) and (b). However, we can omit this non-degeneracy. In fact, if the gain and loss is balanced ( $\gamma_1 = \gamma_2 = \gamma$ ), and we consider  $\gamma_{1ex} = \gamma_{2ex} = \gamma/2$ ,  $\epsilon_1 = \epsilon_2 = \epsilon$ , then based on the above derivation, it can be easily obtained that the non-degeneracy of the optical supermodes at the exceptional point can be approximated as

$$\frac{\omega_{o+} - \omega_{o-}}{\gamma} \approx \sqrt{\frac{\Delta_-^3}{\frac{2}{3}\gamma \left( g_{om}^2 \frac{\Omega_2 + \Omega_1}{\Omega_1 \Omega_2} \gamma \epsilon^2 \right)^{2/3}}}, \quad (4)$$

thus when

$$\Delta_- \ll \sqrt[3]{\frac{2}{3}\gamma \left( g_{om}^2 \frac{\Omega_2 + \Omega_1}{\Omega_1 \Omega_2} \gamma \epsilon^2 \right)^2}, \quad (5)$$

this non-degeneracy will be very small, and the purely optical part of the system can be approximated as a  $\mathcal{PT}$ -symmetric structure. Hence, we treat this purely optical structure as an approximate  $\mathcal{PT}$ -symmetric structure in our work.

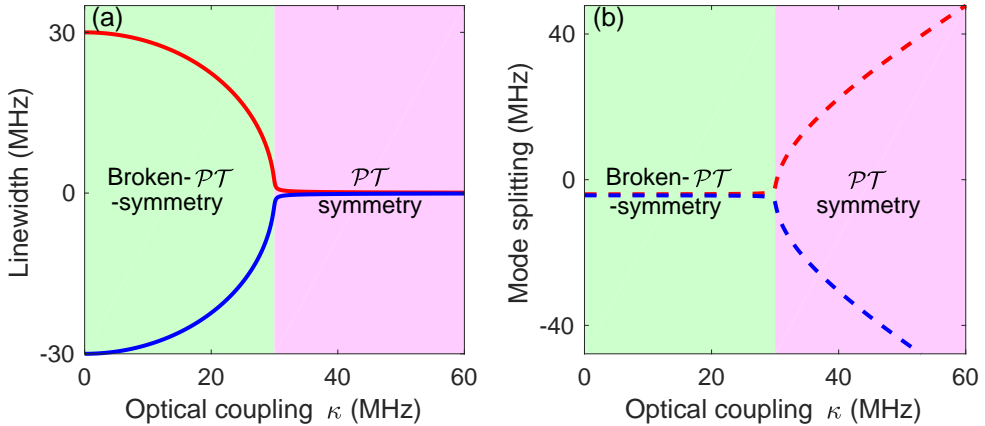


FIG. 1: (Color online) (a) Linewidth of the supermodes, i.e., the real parts of the eigenfrequencies, (b) mode splitting of the supermodes, i.e., the imaginary parts of the eigenfrequencies. The green region is the broken- $\mathcal{PT}$ -symmetry regime, the pink region corresponds to the  $\mathcal{PT}$ -symmetry regime.

### B. Indirectly coupled resonators by add-drop fibers

From the above analysis, we know that if the two directly coupled micro-resonators in our system have balanced loss and gain, i.e.,  $\gamma_1 = \gamma_2 = \gamma$ , and considering the case of critical coupling such that  $\gamma_{1ex} = \gamma_{2ex} = \gamma/2$ , there exists an exceptional point at  $\kappa_{EP} = \gamma$  in our system, and we can enter the  $\mathcal{PT}$ -symmetric regime when  $\kappa > \kappa_{EP}$  (see, e.g., the experimental results in Ref. [1]).

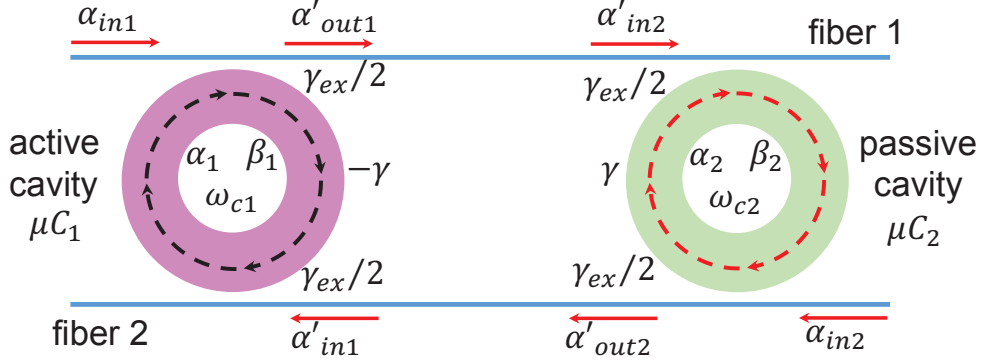


FIG. 2: (Color online) An active resonator indirectly couples with a passive resonator through two optical fibers.

However, if these two optical resonators are not directly coupled with each other. Instead, for example, they are indirectly coupled through add-drop optical fibers, as shown in Fig. 2. Then the optical coupling strength between the two resonators cannot be larger than the external damping rate of each resonator, and thus the system cannot enter the  $\mathcal{PT}$ -symmetric regime. To show this, let us see that dynamical equations of the system described in Fig. 2 can be expressed as

$$\begin{aligned}\dot{\alpha}_1 &= (\gamma_1 - i\Delta_1)\alpha_1 - ig_{om}\alpha_1(\beta_1 + \beta_1^*) + \sqrt{\gamma_{ex}}\alpha_{in1} + \sqrt{\gamma_{ex}}\alpha'_{in1}, \\ \dot{\alpha}_2 &= -(\gamma_2 + i\Delta_2)\alpha_2 - ig_{om}\alpha_2(\beta_2 + \beta_2^*) + \sqrt{\gamma_{ex}}\alpha_{in2} + \sqrt{\gamma_{ex}}\alpha'_{in2}, \\ \dot{\beta}_1 &= -(\Gamma_{m1} + i\Omega_1)\beta_1 - ig_{om}|\alpha_1|^2, \\ \dot{\beta}_2 &= -(\Gamma_{m2} + i\Omega_2)\beta_2 - ig_{om}|\alpha_2|^2.\end{aligned}\quad (6)$$

From the input-output theory [2], we know that

$$\begin{aligned}\alpha'_{in1} &= \alpha'_{out2} = \alpha_{in2} - \sqrt{\gamma_{ex}}\alpha_2, \\ \alpha'_{in2} &= \alpha'_{out1} = \alpha_{in1} - \sqrt{\gamma_{ex}}\alpha_1.\end{aligned}\quad (7)$$

By substituting the above equations into Eq. (6), and omitting the optomechanical coupling terms under the condition that  $g_{om} \ll \gamma_i, \Delta_i$ , we can obtain the reduced dynamical equations of the optical modes as

$$\begin{aligned}\dot{\alpha}_1 &\approx [\gamma_1 - i(\Delta_1 + \Delta_{1s})]\alpha_1 + \sqrt{\gamma_{ex}}\alpha_{in1} + \sqrt{\gamma_{ex}}(\alpha_{in2} - \sqrt{\gamma_{ex}}\alpha_2) \\ &\approx (\gamma_1 - i\Delta_1)\alpha_1 - \gamma_{ex}\alpha_2 + \sqrt{\gamma_{ex}}\alpha_{in1} + \sqrt{\gamma_{ex}}\alpha_{in2}, \\ \dot{\alpha}_2 &\approx [-\gamma_2 - i(\Delta_2 + \Delta_{2s})]\alpha_2 + \sqrt{\gamma_{ex}}\alpha_{in2} + \sqrt{\gamma_{ex}}(\alpha_{in1} - \sqrt{\gamma_{ex}}\alpha_1) \\ &\approx -(\gamma_2 + i\Delta_2)\alpha_2 - \gamma_{ex}\alpha_1 + \sqrt{\gamma_{ex}}\alpha_{in1} + \sqrt{\gamma_{ex}}\alpha_{in2}.\end{aligned}\quad (8)$$

Here, we consider the case that loss and gain are balanced ( $\gamma_1 = \gamma_2 = \gamma$ ), and  $\Delta_1 = \Delta_2$ . Then the above dynamical equation Eq. (6) can be reduced to

$$\begin{aligned}\dot{\alpha}_1 &\approx (\gamma - i\Delta)\alpha_1 - \gamma_{ex}\alpha_2 + \sqrt{\gamma_{ex}}\alpha_{in1} + \sqrt{\gamma_{ex}}\alpha_{in2}, \\ \dot{\alpha}_2 &\approx -(\gamma + i\Delta)\alpha_2 - \gamma_{ex}\alpha_1 + \sqrt{\gamma_{ex}}\alpha_{in1} + \sqrt{\gamma_{ex}}\alpha_{in2}.\end{aligned}\quad (9)$$

It can be seen that the optical coupling strength between the two resonators is  $\kappa = \gamma_{ex}$ . This means that, in this case, the optical coupling strength cannot be larger than the external damping rate  $\gamma_{ex}$  of each resonator, thus the system also cannot enter the  $\mathcal{PT}$ -symmetric regime since  $\kappa = \gamma_{ex} < \gamma$ .

### C. The derivation of the reduced dynamical equation of the mechanical modes

Based on the dynamical equation in Eq. (1), we can adiabatically eliminate the degrees of freedom of the optical modes, and derive the reduced dynamical equations of the mechanical modes. In fact, by rewriting the first two equations in Eq. (1) in matrix format, we have

$$\begin{bmatrix} \dot{\alpha}_1 \\ \dot{\alpha}_2 \end{bmatrix} = M \begin{bmatrix} \alpha_1 \\ \alpha_2 \end{bmatrix} + \begin{bmatrix} -ig_{om}\alpha_1(\beta_1 + \beta_1^*) \\ -ig_{om}\alpha_2(\beta_2 + \beta_2^*) \end{bmatrix} + \begin{bmatrix} \sqrt{2\gamma_{1ex}}\epsilon_1 \\ \sqrt{2\gamma_{2ex}}\epsilon_2 \end{bmatrix}, \quad (10)$$

where

$$M = \begin{bmatrix} \gamma_1 - i\Delta_1 & -i\kappa \\ -i\kappa & -\gamma_2 - i\Delta_2 \end{bmatrix}.$$

The matrix  $M$  can be diagonalized as

$$M = T\Lambda T^{-1},$$

where

$$\Lambda = \begin{bmatrix} \omega_+ & 0 \\ 0 & \omega_- \end{bmatrix}, T = \begin{bmatrix} \tau_+ & \tau_- \\ 1 & 1 \end{bmatrix},$$

and

$$\begin{aligned} \omega_+ &= \frac{\gamma_1 - \gamma_2}{2} - i\frac{\Delta_1 + \Delta_2}{2} - i\sqrt{\kappa^2 + \left(\frac{\Delta_1 - \Delta_2}{2} + i\frac{\gamma_1 + \gamma_2}{2}\right)^2}, \\ \omega_- &= \frac{\gamma_1 - \gamma_2}{2} - i\frac{\Delta_1 + \Delta_2}{2} + i\sqrt{\kappa^2 + \left(\frac{\Delta_1 - \Delta_2}{2} + i\frac{\gamma_1 + \gamma_2}{2}\right)^2}, \\ \tau_+ &= \frac{\Delta_1 - \Delta_2 + i(\gamma_1 + \gamma_2)}{2\kappa} + \sqrt{1 + \left(\frac{\Delta_1 - \Delta_2 + i(\gamma_1 + \gamma_2)}{2\kappa}\right)^2}, \\ \tau_- &= \frac{\Delta_1 - \Delta_2 + i(\gamma_1 + \gamma_2)}{2\kappa} - \sqrt{1 + \left(\frac{\Delta_1 - \Delta_2 + i(\gamma_1 + \gamma_2)}{2\kappa}\right)^2}. \end{aligned}$$

Thus, we can introduce the following optical supermodes

$$\begin{bmatrix} \alpha_+ \\ \alpha_- \end{bmatrix} = T^{-1} \begin{bmatrix} \alpha_1 \\ \alpha_2 \end{bmatrix}, \quad (11)$$

by which Eq. (10) can be reexpressed as

$$\begin{bmatrix} \dot{\alpha}_+ \\ \dot{\alpha}_- \end{bmatrix} = \begin{bmatrix} \omega_+ & 0 \\ 0 & \omega_- \end{bmatrix} \begin{bmatrix} \alpha_+ \\ \alpha_- \end{bmatrix} - ig_{om} \begin{bmatrix} (\lambda_+ \alpha_+ + \lambda_- \alpha_-)(\beta_1 + \beta_1^*) - \lambda_-(\alpha_+ + \alpha_-)(\beta_2 + \beta_2^*) \\ -(\lambda_+ \alpha_+ + \lambda_- \alpha_-)(\beta_1 + \beta_1^*) + \lambda_+(\alpha_+ + \alpha_-)(\beta_2 + \beta_2^*) \end{bmatrix} + \begin{bmatrix} \mu \sqrt{2\gamma_{1ex}}\epsilon_1 - \lambda_- \sqrt{2\gamma_{2ex}}\epsilon_2 \\ -\mu \sqrt{2\gamma_{1ex}}\epsilon_1 + \lambda_+ \sqrt{2\gamma_{2ex}}\epsilon_2 \end{bmatrix},$$

where

$$\begin{aligned} \lambda_- &= \frac{\Delta_1 - \Delta_2 + i(\gamma_1 + \gamma_2) - \sqrt{4\kappa^2 + (\Delta_1 - \Delta_2 + i(\gamma_1 + \gamma_2))^2}}{2\sqrt{4\kappa^2 + (\Delta_1 - \Delta_2 + i(\gamma_1 + \gamma_2))^2}}, \\ \lambda_+ &= \frac{\Delta_1 - \Delta_2 + i(\gamma_1 + \gamma_2) + \sqrt{4\kappa^2 + (\Delta_1 - \Delta_2 + i(\gamma_1 + \gamma_2))^2}}{2\sqrt{4\kappa^2 + (\Delta_1 - \Delta_2 + i(\gamma_1 + \gamma_2))^2}}, \\ \mu &= \frac{\kappa}{\sqrt{4\kappa^2 + (\Delta_1 - \Delta_2 + i(\gamma_1 + \gamma_2))^2}}. \end{aligned}$$

To adiabatically eliminate the degrees of freedom of the optical modes, we let  $\dot{\alpha}_+ = \dot{\alpha}_- = 0$ , by which we can obtain the following stationary solution

$$\begin{aligned}\alpha_{+ss} &= \frac{-\mu(\omega_- - ig_{om}(\beta_2 + \beta_2^*))\sqrt{2\gamma_{1ex}}\epsilon_1 + \lambda_-(\omega_- - ig_{om}(\beta_1 + \beta_1^*))\sqrt{2\gamma_{2ex}}\epsilon_2}{\omega_+\omega_- + ig_{om}(\omega_+\lambda_- - \omega_-\lambda_+)(\beta_1 + \beta_1^*) + ig_{om}(-\omega_+\lambda_+ + \omega_-\lambda_-)(\beta_2 + \beta_2^*) - g_{om}^2(\lambda_+ - \lambda_-)^2(\beta_1 + \beta_1^*)(\beta_2 + \beta_2^*)}, \\ \alpha_{-ss} &= \frac{\mu(\omega_+ - ig_{om}(\beta_2 + \beta_2^*))\sqrt{2\gamma_{1ex}}\epsilon_1 - \lambda_+(\omega_+ - ig_{om}(\beta_1 + \beta_1^*))\sqrt{2\gamma_{2ex}}\epsilon_2}{\omega_+\omega_- + ig_{om}(\omega_+\lambda_- - \omega_-\lambda_+)(\beta_1 + \beta_1^*) + ig_{om}(-\omega_+\lambda_+ + \omega_-\lambda_-)(\beta_2 + \beta_2^*) - g_{om}^2(\lambda_+ - \lambda_-)^2(\beta_1 + \beta_1^*)(\beta_2 + \beta_2^*)}.\end{aligned}\quad (12)$$

By introducing the power-series expansion and omitting high-order terms of  $\beta_1$  and  $\beta_2$  ( $g_{om} \ll |\Delta_2 - \Delta_1|$ ), the above solutions can be simplified as

$$\begin{aligned}\alpha_{+ss} &\approx -\frac{\mu\sqrt{2\gamma_{1ex}}\epsilon_1 - \lambda_-\sqrt{2\gamma_{2ex}}\epsilon_2}{\omega_+} \\ &\quad + ig_{om}\frac{\omega_-(\mu\sqrt{2\gamma_{1ex}}\epsilon_1 - \lambda_-\sqrt{2\gamma_{2ex}}\epsilon_2)(\omega_+\lambda_- - \omega_-\lambda_+) - \lambda_-\omega_+\omega_-\sqrt{2\gamma_{2ex}}\epsilon_2}{(\omega_+\omega_-)^2}(\beta_1 + \beta_1^*) \\ &\quad + ig_{om}\frac{\omega_-(\mu\sqrt{2\gamma_{1ex}}\epsilon_1 - \lambda_-\sqrt{2\gamma_{2ex}}\epsilon_2)(-\omega_+\lambda_+ + \omega_-\lambda_-) + \mu\omega_+\omega_-\sqrt{2\gamma_{1ex}}\epsilon_1}{(\omega_+\omega_-)^2}(\beta_2 + \beta_2^*), \\ \alpha_{-ss} &\approx -\frac{\mu\sqrt{2\gamma_{1ex}}\epsilon_1 - \lambda_+\sqrt{2\gamma_{2ex}}\epsilon_2}{\omega_-} \\ &\quad + ig_{om}\frac{\omega_+(\mu\sqrt{2\gamma_{1ex}}\epsilon_1 - \lambda_+\sqrt{2\gamma_{2ex}}\epsilon_2)(\omega_+\lambda_- - \omega_-\lambda_+) - \lambda_+\omega_+\omega_-\sqrt{2\gamma_{2ex}}\epsilon_2}{(\omega_+\omega_-)^2}(\beta_1 + \beta_1^*) \\ &\quad + ig_{om}\frac{\omega_+(\mu\sqrt{2\gamma_{1ex}}\epsilon_1 - \lambda_+\sqrt{2\gamma_{2ex}}\epsilon_2)(-\omega_+\lambda_+ + \omega_-\lambda_-) + \mu\omega_+\omega_-\sqrt{2\gamma_{1ex}}\epsilon_1}{(\omega_+\omega_-)^2}(\beta_2 + \beta_2^*).\end{aligned}\quad (13)$$

Thus, the stationary solutions of  $\alpha_1$  and  $\alpha_2$  can be expressed as

$$\begin{aligned}\alpha_{1ss} &= \tau_+\alpha_{+ss} + \tau_-\alpha_{-ss} \\ &= \frac{\sigma_2\sqrt{2\gamma_{1ex}}\epsilon_1 - i\kappa\sqrt{2\gamma_{2ex}}\epsilon_2}{\kappa^2 + \delta^2 + \sigma^2} - ig_{om}\frac{\sigma_2^2\sqrt{2\gamma_{1ex}}\epsilon_1 - i\kappa\sigma_2\sqrt{2\gamma_{2ex}}\epsilon_2}{\kappa^2 + \delta^2 + \sigma^2}(\beta_1 + \beta_1^*) \\ &\quad + ig_{om}\frac{\kappa^2\sqrt{2\gamma_{1ex}}\epsilon_1 + i\kappa\sigma_1\sqrt{2\gamma_{2ex}}\epsilon_2}{\kappa^2 + \delta^2 + \sigma^2}(\beta_2 + \beta_2^*), \\ \alpha_{2ss} &= \alpha_{+ss} + \alpha_{-ss} \\ &= \frac{-i\kappa\sqrt{2\gamma_{1ex}}\epsilon_1 + \sigma_1\sqrt{2\gamma_{2ex}}\epsilon_2}{\kappa^2 + \delta^2 + \sigma^2} + ig_{om}\frac{i\kappa\sigma_2\sqrt{2\gamma_{1ex}}\epsilon_1 + \kappa^2\sqrt{2\gamma_{2ex}}\epsilon_2}{\kappa^2 + \delta^2 + \sigma^2}(\beta_1 + \beta_1^*) \\ &\quad - ig_{om}\frac{-i\kappa\sigma_1\sqrt{2\gamma_{1ex}}\epsilon_1 + \sigma_1^2\sqrt{2\gamma_{2ex}}\epsilon_2}{\kappa^2 + \delta^2 + \sigma^2}(\beta_2 + \beta_2^*),\end{aligned}\quad (14)$$

where

$$\begin{aligned}\sigma_1 &= -\gamma_1 + i\Delta_1, \quad \sigma_2 = \gamma_2 + i\Delta_2, \\ \delta &= \frac{\Delta_1 - \Delta_2}{2} + i\frac{\gamma_1 + \gamma_2}{2}, \quad \sigma = \frac{-\gamma_1 + \gamma_2}{2} + i\frac{\Delta_1 + \Delta_2}{2}.\end{aligned}$$

By substituting the above stationary solution into the dynamical equations of the mechanical modes  $\beta_1$  and  $\beta_2$  in Eq. (1), and dropping the counter-rotating terms with  $\beta_{1,2}^*$ , the dynamical equation of reduced mechanical system can be expressed in the matrix format as

$$\begin{bmatrix} \dot{\beta}_1 \\ \dot{\beta}_2 \end{bmatrix} = \begin{bmatrix} -\Gamma_{m1} - i(\Omega_1 + \delta\Omega_1) & -i\kappa_m \\ -i\kappa_m & -\Gamma_{m2} - i(\Omega_2 + \delta\Omega_2) \end{bmatrix} \begin{bmatrix} \beta_1 \\ \beta_2 \end{bmatrix} - \begin{bmatrix} i\eta_1 \\ i\eta_2 \end{bmatrix}, \quad (15)$$

where

$$\begin{aligned}
\delta\Omega_1 &= \frac{4g_{om}^2 [(\kappa^2 - \Delta_1\Delta_2)\Delta_2 - \Delta_1\gamma_2^2] [\gamma_2^2\gamma_{1ex}\epsilon_1^2 + (\Delta_2\sqrt{\gamma_{1ex}}\epsilon_1 - \kappa\sqrt{\gamma_{2ex}}\epsilon_2)^2]}{[(\kappa^2 - \Delta_1\Delta_2 - \gamma_1\gamma_2)^2 + (\Delta_1\gamma_2 - \Delta_2\gamma_1)^2]^2}, \\
\delta\Omega_2 &= \frac{4g_{om}^2 [(\kappa^2 - \Delta_1\Delta_2)\Delta_1 - \Delta_2\gamma_1^2] [\gamma_1^2\gamma_{2ex}\epsilon_2^2 + (\kappa\sqrt{\gamma_{1ex}}\epsilon_1 - \Delta_1\sqrt{\gamma_{2ex}}\epsilon_2)^2]}{[(\kappa^2 - \Delta_1\Delta_2 - \gamma_1\gamma_2)^2 + (\Delta_1\gamma_2 - \Delta_2\gamma_1)^2]^2}, \\
\kappa_m &= 4ig_{om}^2\kappa \left\{ \frac{\kappa\gamma_{1ex}\epsilon_1^2 [\Delta_2(\kappa^2 - \Delta_1\Delta_2 - 2\gamma_1\gamma_2) + \Delta_1\gamma_2^2] + \kappa\gamma_{2ex}\epsilon_2^2 [\Delta_1(\kappa^2 - \Delta_1\Delta_2) - \Delta_2\gamma_1^2]}{[(\kappa^2 - \Delta_1\Delta_2 - \gamma_1\gamma_2)^2 + (\Delta_1\gamma_2 - \Delta_2\gamma_1)^2]^2} \right. \\
&\quad \left. - \frac{\sqrt{\gamma_{1ex}\gamma_{2ex}}\epsilon_1\epsilon_2 [(\kappa^2 - \gamma_1\gamma_2)^2 - \Delta_1^2\Delta_2^2 - (\Delta_1^2\gamma_2^2 - \Delta_2^2\gamma_1^2)]}{[(\kappa^2 - \Delta_1\Delta_2 - \gamma_1\gamma_2)^2 + (\Delta_1\gamma_2 - \Delta_2\gamma_1)^2]^2} \right\}, \\
\eta_1 &= \frac{g_{om} [\gamma_2^2\epsilon_1^2 + (\Delta_2\epsilon_1 - \kappa\epsilon_2)^2]}{(\kappa^2 - \Delta_1\Delta_2 - \gamma_1\gamma_2)^2 + (\Delta_1\gamma_2 - \Delta_2\gamma_1)^2}, \\
\eta_2 &= \frac{g_{om} [\gamma_1^2\epsilon_2^2 + (\kappa\epsilon_1 - \Delta_1\epsilon_2)^2]}{(\kappa^2 - \Delta_1\Delta_2 - \gamma_1\gamma_2)^2 + (\Delta_1\gamma_2 - \Delta_2\gamma_1)^2}. \tag{16}
\end{aligned}$$

#### D. The optomechanics-induced effective mechanical frequency shifts and mechanical coupling

Let us assume that the gain and loss are well-balanced such that  $\gamma_1 = \gamma_2 \equiv \gamma$  and consider the critical coupling case such that  $\gamma_{1ex} = \gamma_{2ex} = \gamma/2$ . When  $g_{om} \ll |\Delta_1 - \Delta_2| \ll \kappa, \gamma$  and  $\epsilon_1 = \epsilon_2 \equiv \epsilon$ , the two mechanical frequency shifts  $\delta\Omega_{1,2}$  can be simplified as

$$\delta\Omega_1 = -\delta\Omega_2 \approx \frac{2g_{om}^2\Delta_- (\gamma^2 + \kappa^2)^2\gamma\epsilon^2}{[(\kappa^2 - \gamma^2)^2 + \gamma^2\Delta_-^2]^2}, \tag{17}$$

where  $\Delta_- = \Delta_2 - \Delta_1$ . From Eq. (17), it can be seen that the mechanical frequency shifts will be greatly improved in the vicinity of EP. Given the system parameters in section IA, we show the optomechanics-induced mechanical frequency shifts  $\delta\Omega_{1,2}$  in Fig. 3 (a). When the system is far away from EP, the mechanical frequency shifts  $\delta\Omega_1$  (red solid line) and  $\delta\Omega_2$  (red dashed line) are very small, and can be omitted in comparison to the mechanical frequencies  $\Omega_{1,2}$ . However, both frequency shifts  $\delta\Omega_1$  and  $\delta\Omega_2$  will be greatly amplified in the vicinity of EP, which will modify the mechanical frequencies  $\Omega_{1,2}$  such that  $\Omega_1 + \delta\Omega_1 = \Omega_2 + \delta\Omega_2$ . As shown in Fig. 3 (a), in the  $\mathcal{PT}$ -symmetric regime of the optical modes, these mechanical frequency shifts are enhanced with the decrease of the optical coupling strength  $\kappa$ , which means that smaller coupling strength  $\kappa$  between two optical modes is better for synchronization. In addition, as shown in Fig. 3 (a), the difference between the detuning frequencies of the two optical modes, i.e.,  $|\Delta_2 - \Delta_1|$ , significantly influences the amplification effects of the mechanical frequency shifts  $\delta\Omega_{1,2}$  when the system is around EP. By fixing  $\Delta_2 = 5$  MHz, we plot the curves of  $\delta\Omega_{1,2}$  for different  $\Delta_1$ . We can see that the mechanical frequency shifts  $\delta\Omega_{1,2}$  are greatly enhanced with the decrease of  $|\Delta_2 - \Delta_1|$  in the vicinity of EP.

Under the assumptions that  $\gamma_1 = \gamma_2 \equiv \gamma$ ,  $\gamma_{1ex} = \gamma_{2ex} = \gamma/2$ ,  $|\Delta_1 - \Delta_2| \ll \kappa, \gamma$ , and  $\epsilon_1 = \epsilon_2 \equiv \epsilon$ , the strength of the effective mechanical coupling can be simplified as

$$\kappa_{\text{mech}} \approx \frac{4g_{om}^2\gamma^3\kappa^2\Delta_-\epsilon^2}{[(\kappa^2 - \gamma^2)^2 + \gamma^2\Delta_-^2]^2}, \tag{18}$$

and thus the effective mechanical coupling will be greatly amplified in the vicinity of EP. We then plot the curves of the effective mechanical coupling strength  $\kappa_{\text{mech}}$  versus the optical coupling strength  $\kappa$  in Fig. 3 (b). Here we also fix  $\Delta_2 = 5$  MHz and tune the detuning frequency  $\Delta_1$ . It can be seen that the effective mechanical coupling strength  $\kappa_{\text{mech}}$  is significantly enhanced in the vicinity of EP. Therefore, in the  $\mathcal{PT}$ -symmetric regime of the optical modes, weaker optical coupling strength leads to stronger effective mechanical coupling strength, and thus may be helpful for the synchronization between the two mechanical modes. It is also shown that the degree of amplification of  $\kappa_{\text{mech}}$  is extensively enhanced with the decreasing of  $|\Delta_2 - \Delta_1|$  in the vicinity of EP.

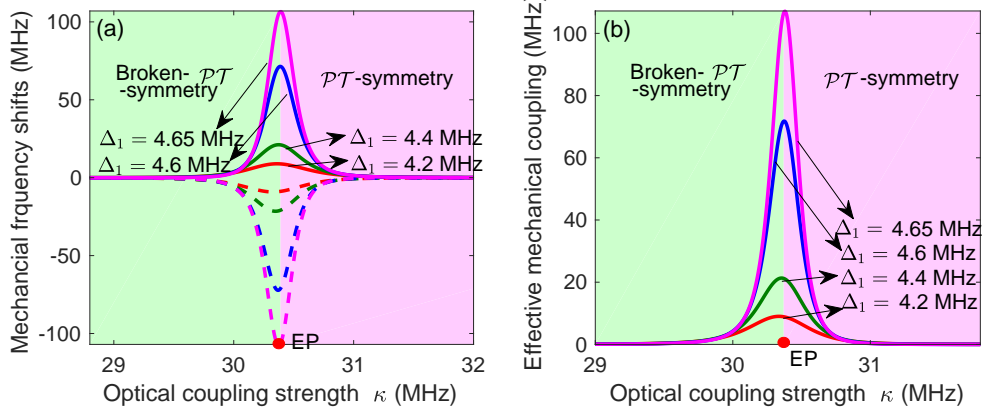


FIG. 3: (Color online) (a) The optomechanics-induced mechanical frequency shifts  $\delta\Omega_{1,2}$  versus the optical coupling strength  $\kappa$  in the broken- $\mathcal{PT}$ -symmetric regime (light green area) and  $\mathcal{PT}$ -symmetric regime (pink area). Here, we fix  $\Delta_2 = 5$  MHz and plot the curves of  $\delta\Omega_{1,2}$  for different  $\Delta_1$ . The solid (dashed) curves denote the curves of the mechanical frequency shift  $\delta\Omega_1$  ( $\delta\Omega_2$ ) with different  $\Delta_1$ . It is shown that  $\delta\Omega_{1,2}$  are greatly amplified in the vicinity of EP and the amplification effects are enhanced with the decrease of  $|\Delta_2 - \Delta_1|$ . (b) The effective mechanical coupling strength  $\kappa_{\text{mech}}$  between the two mechanical modes versus the optical coupling strength  $\kappa$ . Here, we fix  $\Delta_2 = 5$  MHz and plot the curves of  $\kappa_{\text{mech}}$  for different  $\Delta_1$ . It can be seen that  $\kappa_{\text{mech}}$  is also significantly amplified in the vicinity of EP and the amplification effects are improved with the decrease of  $|\Delta_2 - \Delta_1|$ .

#### E. The influence of the effective mechanical coupling on synchronization

In this part we discuss the positive effect of the enhancement of the effective mechanical coupling  $\kappa_{\text{mech}}$  on the synchronization between mechanical modes, i.e., the stronger the  $\kappa_{\text{mech}}$  is, the easier the synchronization is. For simplicity and clarity, we re-express the dynamical equation in Eq. (15) by using the differential operator format as follows

$$\begin{aligned} [\mathcal{D} + (\Gamma_{m1} + i(\Omega_1 + \delta\Omega_1))] \beta_1 - i\kappa_m \beta_2 &= -i\eta_1, \\ -i\kappa_m \beta_1 + [\mathcal{D} + (\Gamma_{m2} + i(\Omega_2 + \delta\Omega_2))] \beta_2 &= -i\eta_2, \end{aligned}$$

where  $\mathcal{D}$  represents the differential operator. By eliminating the degree of freedom of  $\beta_2$ , we can derive the dynamical equation of  $\beta_1$ , and then obtain the characteristic equation of this coupled system as follows

$$\lambda^2 + [\Gamma_{m1} + \Gamma_{m2} + i(\Omega_1 + \delta\Omega_1 + \Omega_2 + \delta\Omega_2)] \lambda + [\Gamma_{m1} + i(\Omega_1 + \delta\Omega_1)] [\Gamma_{m2} + i(\Omega_2 + \delta\Omega_2)] - \kappa_{\text{mech}}^2 = 0.$$

Here, we consider  $\Gamma_{m1} = \Gamma_{m2}$ . Thus the roots of this characteristic equation can be expressed as

$$\begin{aligned} \lambda_+ &= -\frac{\Gamma_{m1} + \Gamma_{m2}}{2} - i\Omega_{Ave+} + i\sqrt{\Omega_{Ave-}^2 - \kappa_{\text{mech}}^2}, \\ \lambda_- &= -\frac{\Gamma_{m1} + \Gamma_{m2}}{2} - i\Omega_{Ave+} - i\sqrt{\Omega_{Ave-}^2 - \kappa_{\text{mech}}^2}, \end{aligned} \quad (19)$$

where

$$\Omega_{Ave+} = \frac{\Omega_1 + \delta\Omega_1 + \Omega_2 + \delta\Omega_2}{2}, \quad \Omega_{Ave-} = \frac{\Omega_1 + \delta\Omega_1 - \Omega_2 - \delta\Omega_2}{2}.$$

It can be easily seen that in the weak coupling regime such that  $\kappa_{\text{mech}} < \Omega_{Ave-}$ , the vibration frequencies of the mechanical modes  $\beta_{1,2}$  are close to each other with the increase of the effective coupling strength  $\kappa_{\text{mech}}$ , which means that the degree of synchronization between the two mechanical modes increases with the increase of  $\kappa_{\text{mech}}$ . At the critical point such that  $\kappa_{\text{mech}} = \Omega_{Ave-}$ , the two oscillators will have the same vibration frequency  $\Omega_{Ave+}$ , which means that these two mechanical modes are with frequency synchronization, i.e., the frequencies of the two mechanical modes are equal to each other. It is shown that a stronger effective mechanical coupling strength can improve the degree of the synchronization between mechanical modes in our system, and finally leads to the frequency synchronization when the effective mechanical coupling is strong enough.

It can be further shown that the two mechanical modes can be in a complete synchronization, i.e., the position and speed of these two mechanical modes completely coincide with each other, when the effective mechanical coupling strength  $\kappa_{\text{mech}}$  is strong enough. To show this, we rewrite the dynamical equation (15) as follows

$$\begin{aligned}\dot{\beta}_1 &= -\Gamma_m \beta_1 - i\Omega_m \beta_1 - i\kappa_m \beta_2, \\ \dot{\beta}_2 &= -\Gamma_m \beta_2 - i\Omega_m \beta_2 - i\kappa_m \beta_1,\end{aligned}\quad (20)$$

Let us then define  $e_- = \beta_1 - \beta_2$ , thus the dynamical equation of  $e_-$  can be expressed as

$$\dot{e}_- = -\Gamma_m e_- - i(\Omega_m - \kappa_m)e_-.\quad (21)$$

It can be shown from the above equation that  $e_- = \beta_1 - \beta_2$  tends to zero when the time tends to infinity. Note that the real parts and the imaginary parts of  $\beta_1$  and  $\beta_2$  are the positions and momenta of the corresponding mechanical resonators. Thus, we can see that the positions and momenta of the two mechanical resonators coincide with each other in the long time limit, which means that the two mechanical resonators are with complete synchronization.

#### F. The enhancement of the effective optomechanical interaction

In our  $\mathcal{PT}$ -symmetric optomechanical system, there exists an enhancement of the effective optomechanical interaction due to the topological-singularity-induced amplification of optomechanical nonlinearity in the vicinity of the exceptional point [5]. This enhanced optomechanical interaction then leads to the amplifications of the optomechanics-induced mechanical frequency shifts  $\delta\Omega_{1,2}$  and the effective mechanical coupling strength  $\kappa_{\text{mech}}$ . Since the optomechanics-induced mechanical frequency shifts can directly change the frequency of the mechanical modes, and the increased effective mechanical coupling can also benefit the synchronization of the mechanical modes, thus the synchronization between far-off-resonant mechanical modes can be realized with sufficiently large optomechanical interaction strength. In the  $\mathcal{PT}$ -symmetric regime, the system approaches to the exceptional point with the decrease of optical coupling strength  $\kappa$ , which results in an enhancement of the optomechanical coupling and thus compensates the reduction of the optical coupling strength. In the following part of this subsection, we will discuss this enhanced effective optomechanical interaction in our  $\mathcal{PT}$ -symmetric optomechanical system.

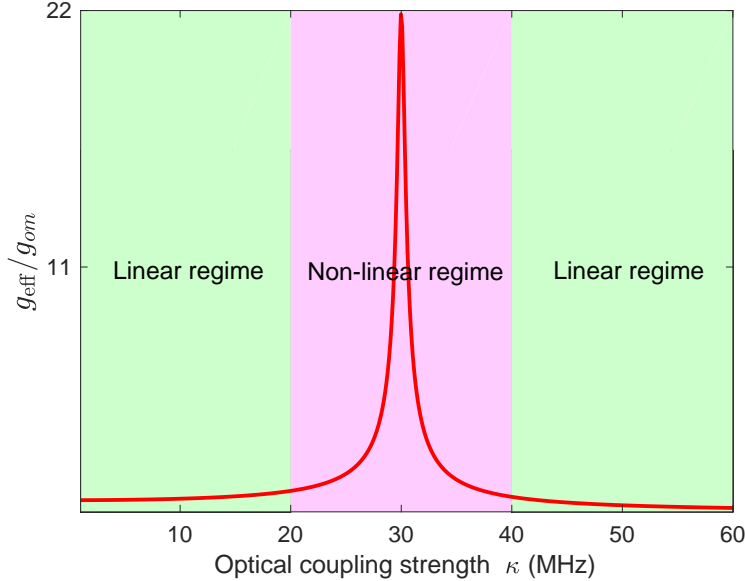


FIG. 4: (Color online) The effective optomechanical coupling strength  $g_{\text{eff}}$  versus the optical coupling strength  $\kappa$ . In the green area, the system is far away from EP, and the effective optomechanical coupling strength  $g_{\text{eff}}$  is linearly dependent on  $\kappa$ . In the pink area, the system is in the vicinity of EP, and in this case,  $g_{\text{eff}}$  changes nonlinearly with  $\kappa$ .

In our optomechanical system, the interaction Hamiltonian between optical modes and mechanical modes can be expressed as

$$H_{\text{int}} = g_{\text{om}} a_1^\dagger a_1 (b_1^\dagger + b_1) + g_{\text{om}} a_2^\dagger a_2 (b_2^\dagger + b_2),\quad (22)$$

where  $a_1$  ( $a_2$ ) and  $b_1$  ( $b_2$ ) represent the annihilation operator of the optical mode and mechanical mode in the active (passive) resonator, respectively, and  $g_{om}$  is the optomechanical coupling strength. If we re-write this interaction Hamiltonian  $H_{int}$  in the optical supermodes picture, then the effective optomechanical coupling strength  $g_{eff}$  between optical supermodes and mechanical modes can be expressed as

$$g_{eff} \approx \frac{g_{om}}{2} \frac{\gamma^2 + \sqrt{(\kappa^2 - \gamma^2)^2 + \gamma^2 \Delta_-^2}}{\sqrt{(\kappa^2 - \gamma^2)^2 + \gamma^2 \Delta_-^2}}. \quad (23)$$

Since  $\Delta_- = |\Delta_2 - \Delta_1| \ll \kappa, \gamma$ , the effective optomechanical coupling strength  $g_{eff}$  can be greatly amplified in the vicinity of EP when  $\kappa \rightarrow \gamma$ . This means that in this case the effective optomechanical coupling strength  $g_{eff}$  can be greatly enhanced. Given the parameters in section IA, we can obtain the simulation results of the effective optomechanical coupling strength  $g_{eff}$  versus the optical coupling strength  $\kappa$ , as shown in Fig. 4. When the optical coupling strength  $\kappa$  is far away from the exceptional point, i.e., in the green area in Fig. 4, the effective optomechanical coupling strength changes linearly with the optical coupling strength  $\kappa$ . However, in the pink area,  $g_{eff}$  increases very fast when the system approaches to EP, which means that in this regime the optomechanical interaction can be greatly amplified. In addition, by comparing Eq. (23) with Eq. (17) and Eq. (18), we can find that  $|\delta\Omega_{1,2}| \propto g_{eff}^4 |f_1(\kappa, \gamma, \epsilon, g_{om}, \Delta_-)|$ , and  $\kappa_{mech} \propto g_{eff}^4 |f_2(\kappa, \gamma, \epsilon, g_{om}, \Delta_-)|$ , which means that the enhanced optomechanical coupling strength can lead to improvements of the optomechanics-induced mechanical frequency shifts and the effective mechanical coupling in the vicinity of EP.

#### G. The difference between active $\mathcal{PT}$ -symmetric system and passive system with EP for synchronization

Based on the previous discussion, we know that in the discussed gain-loss balanced  $\mathcal{PT}$ -symmetric optomechanical system, there exists amplifications of the optomechanics-induced mechanical frequency shifts and effective mechanical coupling strength in the vicinity of exceptional point. However, if this  $\mathcal{PT}$ -symmetric system is replaced by a passive coupled system with an exceptional point, i.e., the active resonator in the discussed  $\mathcal{PT}$ -symmetric system is replaced by a passive resonator, the two far-detuned mechanical modes in this system cannot synchronize with each other. To show this, we can easily obtain the dynamical equations of the system by replacing the optical damping  $\gamma_1$  in Eq. (1) with  $-\gamma_1$

$$\begin{aligned} \dot{\alpha}_1 &= (-\gamma_1 - i\Delta_1)\alpha_1 - i\kappa\alpha_2 - ig_{om}\alpha_1(\beta_1 + \beta_1^*) + \sqrt{2\gamma_{1ex}}\epsilon_1, \\ \dot{\alpha}_2 &= (-\gamma_2 - i\Delta_2)\alpha_2 - i\kappa\alpha_1 - ig_{om}\alpha_2(\beta_2 + \beta_2^*) + \sqrt{2\gamma_{2ex}}\epsilon_2, \\ \dot{\beta}_1 &= -(\Gamma_{m1} + i\Omega_1)\beta_1 - ig_{om}|\alpha_1|^2, \\ \dot{\beta}_2 &= -(\Gamma_{m2} + i\Omega_2)\beta_2 - ig_{om}|\alpha_2|^2. \end{aligned} \quad (24)$$

Under the assumptions that  $\sqrt{2\gamma_{1ex}}\epsilon_1 = \sqrt{2\gamma_{2ex}}\epsilon_2 = \epsilon$ , and  $\Delta_{1,2}, |\Delta_2 - \Delta_1| \ll \kappa, \gamma_{1,2}$ , the optomechanics-induced mechanical frequency shifts  $\delta\Omega_{1,2}$  and the effective mechanical coupling  $\kappa_{mech}$  can be approximately expressed as

$$\begin{aligned} \delta\Omega_1 &= -\delta\Omega_2 \approx g_{om}^2 \frac{\Delta_- \epsilon^2}{[(\kappa^2 + \gamma_1 \gamma_2) + \Delta_+^2]^2}, \\ \kappa_{mech} &\approx 2g_{om}^2 \frac{\kappa \epsilon^2}{[(\kappa^2 + \gamma_1 \gamma_2) + \Delta_+^2]^2}, \end{aligned} \quad (25)$$

where  $\Delta_+ = (\Delta_1 + \Delta_2)/2$  and  $\Delta_- = \Delta_2 - \Delta_1$ . As  $\Delta_- \ll \kappa, \gamma_{1,2}$  and  $g_{om}$  is very tiny,  $\delta\Omega_{1,2}$  and  $\kappa_{mech}$  are very small. This implies that in this passive system with an exceptional point, the amplifications of mechanical frequency shifts and effective mechanical coupling are not strong enough. Thus these two mechanical modes with far-off-resonant mechanical frequencies cannot be synchronized.

In addition, if the balance between gain and loss is broken in our  $\mathcal{PT}$ -symmetric system, i.e.,  $\Gamma_- = |\gamma_1 - \gamma_2|/2 \neq 0$ , the synchronization between the two mechanical modes will be suppressed. In fact, when the balance between gain and loss is broken, the mechanical frequency shifts  $\delta\Omega_{1,2}$  and the effective mechanical coupling  $\kappa_{mech}$  can be expressed

as

$$\begin{aligned}
\delta\Omega_1 &\approx 2g_{om}^2 \frac{\Delta_-(\kappa^2 + \gamma_2^2)\epsilon^2}{[(\kappa^2 - \gamma_1\gamma_2)^2 + (\gamma_1 + \gamma_2)^2\Delta_-^2/4 + \Gamma_-^2\Delta_+^2]^2}, \\
\delta\Omega_2 &\approx 2g_{om}^2 \frac{\Delta_-(\kappa^2 + \gamma_1^2)\epsilon^2}{[(\kappa^2 - \gamma_1\gamma_2)^2 + (\gamma_1 + \gamma_2)^2\Delta_-^2/4 + \Gamma_-^2\Delta_+^2]^2}, \\
\kappa_{\text{mech}} &\approx 4g_{om}^2 \frac{\Delta_-\kappa^2\gamma_1\gamma_2\epsilon^2}{[(\kappa^2 - \gamma_1\gamma_2)^2 + (\gamma_1 + \gamma_2)^2\Delta_-^2/4 + \Gamma_-^2\Delta_+^2]^2}.
\end{aligned} \tag{26}$$

Therefore, with the increase of  $\Gamma_-$ , the amplification effects of the mechanical frequency shifts and the effective mechanical coupling strength will be suppressed. Given the parameters in section IA, we show the mechanical frequency shifts  $\delta\Omega_{1,2}$  and the effective mechanical coupling strength  $\kappa_{\text{mech}}$  with different  $\Gamma_-$  in Figs. 5 (a), (b), and (c), respectively. It can be clearly seen that the amplifications of the mechanical frequency shifts and the effective mechanical coupling strength are seriously suppressed when  $\Gamma_-$  is large, thus the synchronization between the two mechanical modes with far-off-resonant cannot be realized.

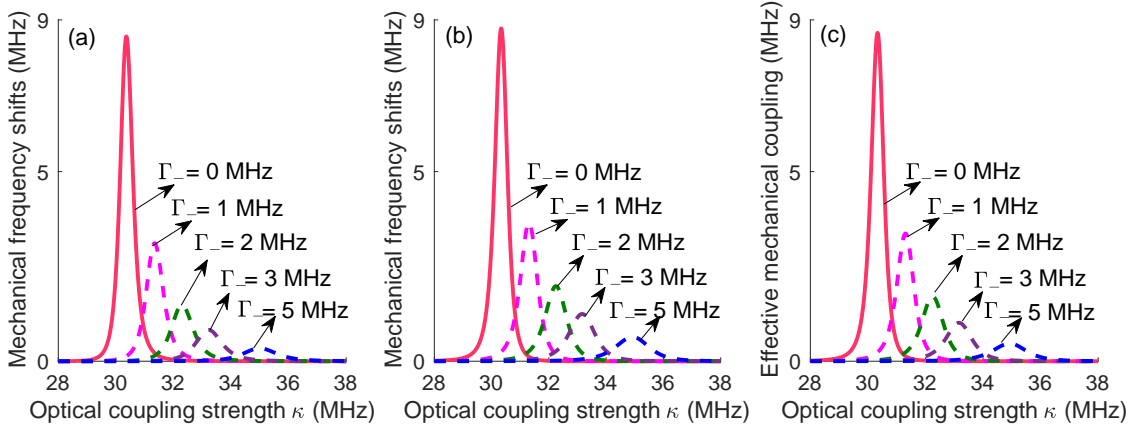


FIG. 5: (Color online) (a) The optomechanics-induced mechanical frequency shifts  $\delta\Omega_1$  versus the optical coupling strength  $\kappa$  with different  $\Gamma_-$ . The solid curve denotes the case that gain and loss are balanced, i.e.,  $\Gamma_- = 0$ . It is shown that the amplification effects of  $\delta\Omega_1$  are suppressed with the increase of  $\Gamma_-$ . (b) Corresponding to the optomechanics-induced mechanical frequency shifts  $-\delta\Omega_2$  versus the optical coupling strength  $\kappa$  with different  $\Gamma_-$ . (c) The effective mechanical coupling  $\kappa_{\text{mech}}$  between the two mechanical modes versus the optical coupling strength  $\kappa$  with different  $\Gamma_-$ . It is shown that the amplification effects of  $\kappa_{\text{mech}}$  are also suppressed with the increase of  $\Gamma_-$

## II. NOISE-ENHANCED SYNCHRONIZATION IN $PT$ -SYMMETRIC OPTOMECHANICAL SYSTEM

### A. Stochastic noises in the optical modes

We then consider the case that there exist white noises in the optical modes. Thus, Eq. (1) can be reexpressed as

$$\begin{aligned}
\dot{\alpha}_1 &= i(\Delta_1 + g_{om}x_1)\alpha_1 + \gamma_1\alpha_1 - i\kappa\alpha_2 + \sqrt{2\gamma_{1ex}}\epsilon_1 + \Gamma_{noise1}(t), \\
\dot{\alpha}_2 &= i(\Delta_2 + g_{om}x_2)\alpha_2 - \gamma_2\alpha_2 - i\kappa\alpha_1 + \sqrt{2\gamma_{2ex}}\epsilon_2 + \Gamma_{noise2}(t), \\
\dot{x}_1 &= -2\Gamma_{m1}\dot{x}_1 - \Omega_1^2x_1 - g_{om}|\alpha_1|^2, \\
\dot{x}_2 &= -2\Gamma_{m2}\dot{x}_2 - \Omega_2^2x_2 - g_{om}|\alpha_2|^2,
\end{aligned} \tag{27}$$

where  $x_i = (\beta_i + \beta_i^*)/2$  is the mechanical displacement of the resonator  $\mu C_i$ .  $\xi_1(t)$  and  $\xi_2(t)$  are two independent identically distributed Gaussian white noises acting on the optical modes  $\alpha_1$  and  $\alpha_2$  satisfying  $\langle \xi_i(t)\xi_j(t+\tau) \rangle = 2D\delta_{ij}\delta(\tau)$ , where  $D$  is the strength of the white noises and  $\langle \cdot \rangle$  is the ensemble average over the stochastic noises. To give more insights for synchronization with noises in our  $\mathcal{PT}$ -symmetric optomechanical system, we show additional

analysis of another index of synchronization—the Kramers rate, which is more suitable to describe noisy synchronized systems.

The Kramers rates of two subsystems are alternative indices to show the correlation between two subsystems. When the Kramers rates of two subsystems coincide with each other, the two subsystems are well correlated [7]. We then calculate the Kramers rates  $r_1$  and  $r_2$  of the mechanical displacements  $x_1$  and  $x_2$ , respectively. The Kramers rate is originally defined as the transition rate between neighboring potential wells of a particle caused by stochastic forces, which was first proposed by Kramers in 1940 [8]. It can be calculated by the following equation [9]

$$r = \frac{\omega_{r1}\omega_{r2}}{2\pi\gamma_v} \exp\left(-\frac{\Delta U}{D}\right), \quad (28)$$

where  $\omega_{r1}^2 = U''(x_a)/m$  is the squared angular frequency at the potential minima  $x_a$  and  $x_c$ , and  $\omega_{r2}^2 = |U''(x_b)|/m$  is the squared angular frequency of the potential at the potential barrier  $x_b$ ,  $U(x)$  and  $\Delta U$  represent the potential of the particle and the height of the potential barrier, respectively, as shown in Fig. 6.  $m$  and  $\gamma_v$  are the mass and the viscous friction of the particle, and  $D$  is the stochastic noise strength. The Kramers rate of the particle is the transition rate between point A and point C (the minimal points of the potential wells) as shown in Fig. 6, and thus is equal to the reciprocal of the transition time  $\tau$  between point A and point C, i.e.,  $r = 1/\tau$ .

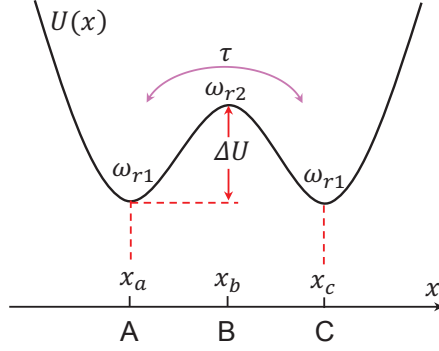


FIG. 6: (Color online) Schematic diagram of the potential energy of a particle. Point A and Point C are the minimal points of the potential wells, and point B is maximal point of the potential barrier. The Kramers rate of the particle is the transition rate between point A and point C, i.e., the reciprocal of the passage time  $\tau$  from point A to point C.

Here, we use the mean first passage time [10, 11], i.e., the average time that the particle moves from one potential well to the other well, to evaluate the Kramers rates  $r_1$  and  $r_2$  of mechanical displacements  $x_1$  and  $x_2$ . We obtain the histograms of  $x_{1,2}$  through numerical simulation first, and then find out the locations  $x_{ia}$  and  $x_{ic}$  ( $i = 1, 2$ ) with the maximum probability of  $x_{1,2}$ , i.e., the potential wells of  $x_{1,2}$ , based on the distribution of histograms, by which we can obtain the mean first passage times  $\tau_{1,2}$ , i.e., the average value of the time intervals between  $x_{ia}$  and  $x_{ic}$ . The Kramers rates  $r_1$  and  $r_2$  can then be calculated by the reciprocal of the mean first passage times  $\tau_{1,2}$ , i.e.,  $r_i = 1/\tau_i$  ( $i = 1, 2$ ). The simulation results for  $r_1$  and  $r_2$  are presented in Fig. 7. In Fig. 7(a), the red solid curve and the blue dashed curve represent the trajectories of  $r_1$  and  $r_2$  with different values of noise intensity  $D$  in the broken- $\mathcal{PT}$ -symmetric regime, where the optical coupling strength is fixed as  $\kappa = 27.76$  MHz. It can be seen that the Kramers rates of mechanical displacements  $x_1$  and  $x_2$  get closer with the increase of the noise intensity  $D$ . In the  $\mathcal{PT}$ -symmetric regime as shown in Fig. 7(b), similar phenomenon can be observed, i.e., the stochastic noises tend to decrease the difference between the Kramers rates  $r_1$  and  $r_2$  when the noise intensity is increased, where the optical coupling strength is fixed as  $\kappa = 32.19$  MHz. These simulation results indicate that the partial frequencies of both mechanical displacements  $x_1$  and  $x_2$  tend to be consistent with each other when more noises are introduced into the  $\mathcal{PT}$ -symmetric optomechanical system. It means that noises can improve the correlation between  $x_1$  and  $x_2$ .

## B. Thermal noises in the mechanical modes

In the above analysis we do not consider the effects of the thermal noises in the mechanical modes. Actually, these thermal noises in the mechanical modes can also benefit the synchronization between the two mechanical modes in our  $\mathcal{PT}$ -symmetric optomechanical system. In order to simplify our discussions, we assume that the thermal noises in the mechanical modes are white noises, based on which the Langevin equation of the mechanical modes can be

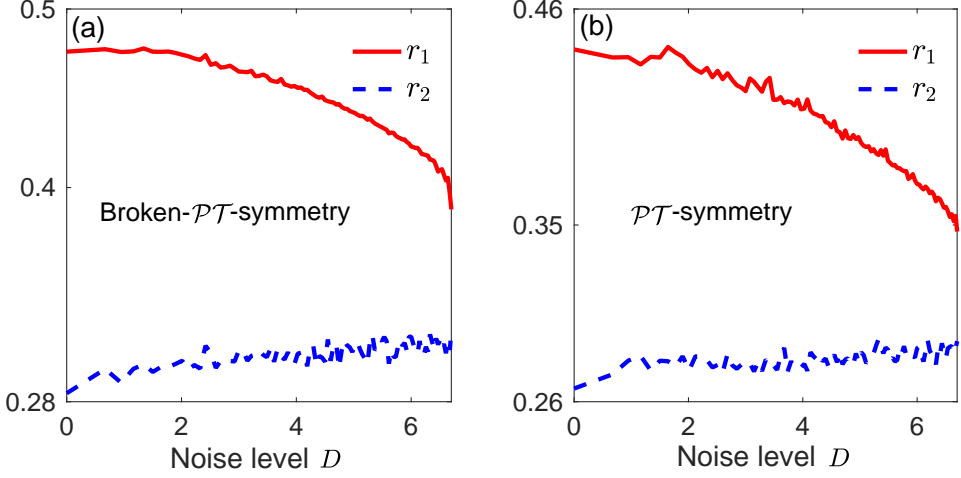


FIG. 7: (Color online) The Kramers rates  $r_1$  and  $r_2$  of mechanical displacements  $x_1$  and  $x_2$  versus the noise intensity  $D$  in broken- $\mathcal{PT}$ -symmetric and  $\mathcal{PT}$ -symmetric regime. (a) The red solid curve (blue dashed curve) represents the curve for Kramers rate  $r_1$  ( $r_2$ ) versus the noise intensity  $D$  in the broken- $\mathcal{PT}$ -symmetric regime. Here the optical coupling strength  $\kappa = 27.76$  MHz is fixed. (b) The red solid curve and blue dashed curve represent the Kramers rates  $r_1$  and  $r_2$  respectively with different stochastic noise intensity  $D$  in the  $\mathcal{PT}$ -symmetric regime, where the optical coupling strength is fixed as  $\kappa = 32.19$  MHz. It can be seen that the Kramers rates  $r_1$  and  $r_2$  get closer with the increase of the noise intensity, which means that the partial frequencies of the mechanical displacements  $x_1$  and  $x_2$  get closer when the noise intensity  $D$  is increased. It means that the stochastic noise can improve the correlation between  $x_1$  and  $x_2$ .

expressed as

$$\begin{aligned}\dot{\beta}_1 &= -\Gamma_m \beta_1 - i\tilde{\Omega}_1 \beta_1 - i\kappa_m \beta_2 + \Gamma_{\text{noise}1}(t), \\ \dot{\beta}_2 &= -\Gamma_m \beta_2 - i\tilde{\Omega}_2 \beta_2 - i\kappa_m \beta_1 + \Gamma_{\text{noise}2}(t),\end{aligned}\quad (29)$$

where  $\Gamma_{\text{noise}1,2}$  are diffusion terms with  $\delta$ -correlated Gaussian distributions, i.e.,

$$\langle \Gamma_{\text{noise } i}(t) \rangle = 0, \quad \langle \Gamma_{\text{noise } i}(t) \Gamma_{\text{noise } j}(t') \rangle = 4\Gamma_m kT \delta(t - t'), \quad (30)$$

where  $k$  is the Boltzman's constant and  $T$  is the temperature.

If we rewrite Eq. (29) by redefining

$$\begin{aligned}\xi_1 &= \frac{\beta_1 + \beta_1^*}{2}, \quad \xi_2 = \dot{\xi}_1, \\ \xi_3 &= \frac{\beta_2 + \beta_2^*}{2}, \quad \xi_4 = \dot{\xi}_2,\end{aligned}\quad (31)$$

we have

$$\begin{aligned}\begin{bmatrix} \dot{\xi}_1(t) \\ \dot{\xi}_2(t) \\ \dot{\xi}_3(t) \\ \dot{\xi}_4(t) \end{bmatrix} &= - \begin{bmatrix} 0 & -1 & 0 & 0 \\ \tilde{\Omega}_1^2 & 2\Gamma_m & \kappa_{\text{mech}} & 0 \\ 0 & 0 & 0 & -1 \\ \kappa_{\text{mech}} & 0 & \tilde{\Omega}_2^2 & 2\Gamma_m \end{bmatrix} \begin{bmatrix} \xi_1(t) \\ \xi_2(t) \\ \xi_3(t) \\ \xi_4(t) \end{bmatrix} + \begin{bmatrix} \Gamma_1 \\ \Gamma_2 \\ \Gamma_3 \\ \Gamma_4 \end{bmatrix} \\ &= -A \begin{bmatrix} \xi_1(t) \\ \xi_2(t) \\ \xi_3(t) \\ \xi_4(t) \end{bmatrix} + \begin{bmatrix} \Gamma_1 \\ \Gamma_2 \\ \Gamma_3 \\ \Gamma_4 \end{bmatrix},\end{aligned}\quad (32)$$

where  $\Gamma_1 = \Gamma_3 = 0$ ;  $\Gamma_2 = \Gamma_{\text{noise}1}$ ; and  $\Gamma_4 = \Gamma_{\text{noise}2}$ . The solution of the above equation can be expressed as

$$\xi_i(t) = \sum_{k=1}^4 G_{ik}(t) z_k + \sum_{k=1}^4 \int_0^t G_{ik}(t') \Gamma_k(t - t') dt', \quad (33)$$

where matrix  $G = (G_{ij}) = \exp(-At)$ , and  $z_i$  represent the initial values of the variables  $\xi_i$ . We then calculate the correlation functions as

$$R_{ij}(\tau, t) = \langle \xi_i(t + \tau) \xi_j(t) \rangle, \quad (34)$$

where  $\langle \cdot \rangle$  is the ensemble average over the stochastic noises. If we assume that the initial time is  $t$ , the solutions of  $\xi_i$  in Eq. (33) can be re-expressed as

$$\xi_i(t + \tau) = \sum_{k=1}^4 G_{ik}(\tau) \xi_i(t) + \sum_{k=1}^4 \int_t^{t+\tau} G_{ik}(t') \Gamma_k(t - t') dt'. \quad (35)$$

Therefore, based on the regression theorem [12], we know that the correlation functions  $R_{ij}(\tau, t)$  can be reduced to

$$R_{ij}(\tau, t) = \sum_{k=1}^4 G_{ik}(\tau) \langle \xi_k(t) \xi_j(t) \rangle, \quad 0 \leq \tau. \quad (36)$$

Considering the short-time limit such that  $t \approx 0$ , the matrix  $G$  can be approximately expressed as

$$\begin{aligned} G(t) &= e^{-At} \\ &\approx I - At \\ &\approx \begin{bmatrix} 1 & t & 0 & 0 \\ -\tilde{\Omega}_1^2 t & 1 - 2\Gamma_m t & -\kappa_{\text{mech}} t & 0 \\ 0 & 0 & 1 & t \\ -\kappa_{\text{mech}} t & 0 & -\tilde{\Omega}_2^2 t & 1 - 2\Gamma_m t \end{bmatrix}. \end{aligned} \quad (37)$$

Thus, the three correlation functions  $R_{13}(\tau, t)$ ,  $R_{11}(0, t)$ , and  $R_{33}(0, t)$  can be expressed as

$$\begin{aligned} R_{13}(\tau, t) &= (z_1 + z_2 t)(z_3 + z_4 t) + \frac{q}{3} t^3 \\ &\quad + \tau \left[ -(\kappa_{\text{mech}} z_3 + \tilde{\Omega}_1^2) (z_3 + z_4 t) + (1 - 2\Gamma_m t)(z_3 + z_4 t) z_2 + \frac{q}{2} t^2 \right], \\ R_{11}(0, t) &= (z_1 + z_2 t)^2 + \frac{q}{3} t^3, \\ R_{33}(0, t) &= (z_3 + z_4 t)^2 + \frac{q}{3} t^3. \end{aligned} \quad (38)$$

For simplicity we assume that the system is stationary at the initial time, i.e.,  $z_2 = z_4 = 0$ , and consider the case that  $z_1 = 1/\tilde{\Omega}_1^2$ ,  $z_3 = 1/\kappa_{\text{mech}}$ , thus the normalized correlation function between the two mechanical modes can be expressed as

$$\begin{aligned} R(\tau, t) &= \frac{|R_{13}(\tau, t)|}{\sqrt{R_{11}(0, t)} \sqrt{R_{33}(0, t)}} \\ &= \frac{\left| 1 - 2\tilde{\Omega}_1^2 \tau t + 4\Gamma_m k T \frac{\kappa_{\text{mech}} \tilde{\Omega}_1^2}{2} \tau t^2 + 4\Gamma_m k T \frac{\kappa_{\text{mech}} \tilde{\Omega}_1^2}{3} \tau t^3 \right|}{\sqrt{1 + \frac{4\Gamma_m k T}{3} \kappa_{\text{mech}}^2 t^3} \sqrt{1 + \frac{4\Gamma_m k T}{3} \tilde{\Omega}_1^4 t^3}} \\ &\approx 1 - 2\tilde{\Omega}_1^2 \tau t + 2\Gamma_m k T \kappa_{\text{mech}} \tilde{\Omega}_1^2 \tau t^2 + \frac{4}{3} \Gamma_m k T \kappa_{\text{mech}} \tilde{\Omega}_1^2 \tau t^3. \end{aligned} \quad (39)$$

It is shown in Eq. (39) that the normalized correlation function  $R$  between the mechanical modes increases with the increase of the strength of the thermal noise, i.e.,  $q = 4\Gamma_m k T$ , which means that the thermal noises in the mechanical modes can benefit the synchronization between the two mechanical modes in our  $\mathcal{PT}$ -symmetric synchronization system.

---

[1] B. Peng, S. K. Özdemir, F. C. Lei, F. Monifi, M. Gianfreda, G. L. Long, S. H. Fan, F. Nori, C. M. Bender, and L. Yang, Parity-time-symmetric whispering-gallery microcavities, *Nat. Phys.* **10**, 394 (2014).

- [2] C. W. Gardiner, and M. J. Collett, Input and output in damped quantum systems: Quantum stochastic differential equations and the master equation, *Phys. Rev. A* **31**, 3761 (1985).
- [3] F. Monifi, J. Zhang, S. K. Özdemir, B. Peng, Y. X. Liu, F. Bo, F. Nori, and L. Yang, Optomechanically induced stochastic resonance and chaos transfer between optical fields, *Nat. Photonics* **10**, 399 (2016).
- [4] Z. P. Liu, J. Zhang, S. K. Özdemir, B. Peng, H. Jing, X. Y. Lü, C. W. Li, L. Yang, F. Nori, and Y. X. Liu, Metrology with PT-symmetric cavities: enhanced sensitivity near the PT-phase transition, *Phys. Rev. Lett.* **117**, 110802 (2016).
- [5] H. Jing, S. K. Özdemir, X. Y. L, J. Zhang, L. Yang, and F. Nori, PT-Symmetric phonon laser, *Phys. Rev. Lett.* **113**, 053604 (2014).
- [6] J. Zhang, B. Peng, S. K. Özdemir, K. Pichler, D. O. Krimer, G. Zhao, F. Nori, Y. X. Liu, S. Rotter, and L. Yang, A phonon laser operating at an exceptional point, *Nat. Photonics* **12**, 479 (2018).
- [7] A. Neiman, Synchronizationlike phenomena in coupled stochastic bistable systems, *Phys. Rev. E* **49**, 3484 (1994).
- [8] H. A. Kramers, Brownian motion in a field of force and the diffusion model of chemical reactions, *Physica* **7**, 284 (1940).
- [9] L. Gammaitoni, P. Hänggi, P. Jung, and F. Marchesoni, Stochastic resonance, *Rev. Mod. Phys.* **70**, 223 (1998).
- [10] G. Klein, Mean first-passage times of Brownian motion and related problems, *R. Soc. London A* **211**, 431 (1952).
- [11] H. Hofmann and F. A. Ivanyuk, Mean first passage time for nuclear fission and the emission of light particles, *Phys. Rev. Lett.* **90**, 132701 (2003).
- [12] H. Risken, *The Fokker-Planck Equation: Methods of Solution and Applications*, 2nd ed. (Springer, Berlin, 1989).